

## A Uniform analysis of the Lyman alpha forest at $z = 0-5$ : III. HST FOS Spectral Atlas.

Jill Bechtold<sup>1</sup>, Adam Dobrzycki<sup>2</sup>,  
Brenda Wilden<sup>1,3</sup>, Miwa Morita<sup>1</sup>, Jennifer Scott<sup>1</sup>, Danuta Dobrzycka<sup>2</sup>, Kim-Vy Tran<sup>1,3</sup>,  
Thomas L. Aldcroft<sup>2</sup>

### ABSTRACT

We analyzed the absorption line spectra of all quasars observed with the high resolution gratings of the *Faint Object Spectrograph* on board the *Hubble Space Telescope*. We examined 788 spectra for 334 quasars, and present line lists and identifications of absorption lines in the spectra of 271 of them. Analysis of the statistics of the Ly- $\alpha$  and metal absorption systems are presented in companion papers (Dobrzycki *et al.* 2001; Scott *et al.* 2001; Morita *et al.* 2001). The data and several analysis products are available electronically and on the authors' web site.

### 1. Introduction

The *Faint Object Spectrograph* (*FOS*, Keyes et al. 1995, and references therein) on board the *Hubble Space Telescope* provided the first opportunity to study quasar spectra in the ultraviolet with sufficient spectral resolution to measure the properties of the narrow absorption lines in detail. The Quasar Absorption Line Key Project used the *FOS* to make a comprehensive study of absorber properties at low and intermediate redshift (Bahcall et al. 1993; Bahcall et al. 1996; Jannuzi et al. 1998, hereafter J98, and references therein). There were many quasars observed with the *FOS*, however, for purposes other than the

---

<sup>1</sup>Steward Observatory, University of Arizona, Tucson, AZ 85721, USA  
e-mail: [jbechtold,jscott]@as.arizona.edu

<sup>2</sup>Harvard-Smithsonian Center for Astrophysics, 60 Garden Street, Cambridge, MA 02138, USA, e-mail: [adobrzycki,ddobrzycka,aldcroft]@cfa.harvard.edu

<sup>3</sup>Present address: Board of Astronomy and Astrophysics, University of California, Santa Cruz, Santa Cruz, CA 95064, USA, e-mail: [bwilden,vy]@ucolick.org

study of their absorption line properties. We have retrieved these data from the Space Telescope Science Institute archive, as well as the original Key Project data, and analyzed the absorption lines in all of the spectra, in a uniform way.

The resulting data set is presented in this paper, and is valuable for many studies. These spectra can be combined with spectra obtained from the ground at moderate resolution (Bechtold 1994, Scott et al. 2000a and references therein), to provide statistics on the Ly- $\alpha$  forest from  $z = 0$  to 5 (Dobrzycki et al. 2001). Although line blending must be accounted for with care, these data are a useful complement to high spectral resolution echelle studies which to date have been carried out on a much smaller number of quasars.

In companion papers, we present a statistical analysis of the Ly- $\alpha$  forest lines (Dobrzycki et al. 2001); we analyze the proximity effect in this sample, in order to derive a limit on the metagalactic ultraviolet background and its evolution (Scott et al. 2001); and analyze the interstellar lines from the Milky Way (Morita et al. 2001). Other topics will be discussed in future papers.

In section 2 we present the data collected from the *HST* archive and describe the data reduction procedure. In section 3 we discuss individual objects. The spectra, continuum fits, linelists, and other analysis products are available electronically and on the authors' web site, described in section 4.

## 2. The data

### 2.1. Reductions

We have collected *HST/FOS* quasar spectra taken with the G130H, G190H, and G270H gratings. To the best of our knowledge, we have obtained all available quasar spectra with these gratings. Table 1 is an abbreviated list of all of the data sets we retrieved. A full list is given in Table 2. Table 2 lists the identification numbers of the individual data sets retrieved from the archive and their dates of observation. Several of the spectra turned out to be of very low quality, or were failed observations, and were not reduced further. Broad absorption line quasars and objects observed in SPECTROPOLARIMETRY mode were not reduced. These are noted in Tables 1 and 2.

Some of the data were retrieved from the archives before the best available calibration products had been applied to the products in the archive. We recalibrated these spectra, using STSDAS. Spectra observed prior to the installation of COSTAR in December 1993 were reduced from raw, uncalibrated data, while for the post-COSTAR observations we

used calibrated images. The new calibration methods available for pre-COSTAR data are mainly concerned with improved scattered light corrections and flux calibration. For all the raw data we applied the *addnewkeys* and *calfos* tasks from the *stdas.hst.calib.fos* package, creating calibrated files containing data similar in format and contents to the post-COSTAR calibrated data. The data that was re-calibrated, and the flatfield files used are listed in Table 2.

We then extracted the data from the reduced images following a procedure dependent on the observation mode. If the spectrum was taken in the RAPID-READOUT mode, we combined the spectra from all groups within the image using the *rcombine* task from the *stdas.hst.calib.ctools* package, propagating the error and data quality flags. If the data were taken in the SPECTROSCOPY mode, the last group in the image is the sum of all groups.

Flux and error spectra of the same object taken in succession with the same observing setup (i.e. having the same detector, observation mode, aperture and disperser) were then combined into a single spectrum, weighting them by the exposure time of each individual spectrum. Several objects were observed more than once with the same grating but with different apertures. For those objects we analyzed the higher signal-to-noise spectrum, which typically was also the higher spectral resolution spectrum. Table 2 notes which data sets were combined into the spectrum we used for the absorption line analysis.

Spectra were dereddened using IRAF task *deredden*, taking as input the HI column density calculated using the COLDEN code, written by J. McDowell, which utilizes data from Stark et al. (1992); for objects with  $\delta < -40^\circ$  we used the data from the galactic reddening map of Burstein & Heiles (1982). Conversion from HI column density to E(B-V) was assumed to be  $N_{HI}/E(B-V)=4.8 \times 10^{21} \text{ cm}^{-2} \text{ magn}^{-1}$  (Bohlin, Savage & Drake 1978). The Milky Way reddening curve of Cardelli, Clayton & Mathis (1989) was assumed. The value of E(B-V) which was used is listed in Table 2.

We put all the spectra and line lists on an absolute wavelength scale where possible by calculating the average offset of the detected Galactic interstellar lines in each spectrum. We looked for the SiII(1190,1193,1260,1526), SiIII(1206), CII(1334), and CIV(1548,1550) absorption in the G130H spectra, the AlII(1670) line in the G190H spectra, and FeII(2344, 2374, 2382, 2586, 2600), MgII(2796,2803), and MgI(2853) lines in the G270H spectra. In several cases, especially for G190H data, no Galactic absorption lines were detected and we then applied no wavelength shift to the spectrum. We list the offsets adopted in Table 2.

The Key Project went to great lengths to identify possible residual flat-field features in their spectra, which would erroneously be identified as absorption lines (see Schneider et al. 1993, J98). We did not attempt to repeat this for all the spectra here. Therefore, there is

a possibility that any particular weak absorption line is not real. In J98, they present 117 non-BAL quasar spectra, and report 88 flatfield features: they found no flatfield features in 10 G130H spectra, 47 flatfield features in 46 G190H spectra and 32 flatfield features in 61 G270H spectra. For most purposes, these features have a small effect statistically on the absorption line sample (see also Dobrzycki et al. 2001).

## 2.2. Absorption Line Analysis

For all spectra we determined signal-to-noise ratios, performed continuum fits, detected absorption lines and identified the metal systems using program FINDSL (Aldcroft, Bechtold, & Elvis 1994). The estimations of equivalent width were done both by direct integration of the profile, and by fitting gaussians. Direct integration overcomes the problem of asymmetric lines which is seen for the large aperture in *FOS*, pre-COSTAR (see section 2.4). In the end, we decided *not* to use these spectra in the subsequent analysis of the absorbers, and so used the equivalent widths from gaussian fits (see Paper IV). We quantified the effect of line blending and completeness by generating simulated data sets, and describe the results in section 2.6.

The significance of each absorption line was estimated in two ways. To search for candidate absorption lines, we ran a boxcar of width equal to 2.46 times the full-width-half-maximum of the spectral line spread function in pixels. We calculated the equivalent width and its error, derived from the straightforward propagation of errors from the errors on the flux in each individual pixel. One measure of the significance of a line is then the ratio of the equivalent width to its error. This underestimates the significance, however, since the signal-to-noise in the bottom of the absorption line is worse than it would have been had the line not been there. We calculated a threshold for detecting lines by calculating the one-sigma error for an absorption line as a function of wavelength for the observed flux and our continuum fit in boxcars of the same width as our search technique (9 pixels for most of the data). To interpolate over the regions where there were actual absorption lines, we fit a spline to the calculated threshold as a function of wavelength and, to be conservative, forced it to outline the upper envelope of the data. Then for each line for which the ratio of equivalent width to its error was greater than 3 after the initial search, we interpolated the spline fits to the threshold files and calculated a significance equal to the ratio of the measured equivalent width to the one-sigma error in the smoothed threshold file. We kept lines where this ratio was greater than  $3.5\sigma$ . The significance derived in this way is reported in the line lists. Any line in these lists is real, but the sample is not complete unless a higher threshold is applied. We discuss completeness in section 2.6.

### 2.3. Identification of Metal Lines

Metal absorption line systems were searched for in a number of ways. First we reviewed the literature and examined all reported redshift systems, using the NASA/IPAC Extragalactic Database (NED) and the York et al. (1991) absorption line catalog. We adopted the search list of strong transitions given by Morton et al. (1988). In a few cases, we decided that redshift systems reported in the literature were spurious; these are noted individually in section 3. We also examined the lines shortward of Ly- $\alpha$  with equivalent widths greater than 1 Å, and tested whether a plausible identification could be made if these lines were Ly- $\alpha$ .

Finally, we used a computer program to search for redshift systems automatically. We used the Morton search list and looked for redshifts which resulted in at least 5 matches in the line lists. We ran the code on simulated Ly- $\alpha$  forest spectra with no metal systems to assess the probability of chance matches in the forest. We found that systems with 4 matches and plausible line ratios were commonly found. We made no assumptions about ion ratios, but did require that all the transitions for a particular ion have physically reasonable equivalent width ratios given the f-values listed in Morton (1991), and that Ly- $\alpha$  be detected if it was in the spectral coverage.

Since our goal was to construct a sample for studying the Ly- $\alpha$  forest, we were generous in our identifications: if there was any doubt, we went ahead and identified a line as a metal transition. We kept track of the regions of the spectrum which contained metal lines, and provide this information electronically. In effect these are parts of the redshift path which were not observed for Ly- $\alpha$  and our analysis programs simply delete these parts of the spectrum automatically. Therefore, before drawing conclusions about any particular line identified as a metal, one should look carefully at all the lines identified for that redshift system.

Note that this data is *not* appropriate for deriving certain types of statistics for the metal-line absorbers. We didn't keep track of why a particular quasar was observed, and clearly some objects were observed because they were known beforehand to have interesting metal-line systems, for example damped Ly- $\alpha$  absorbers.

In Figure 1, we plot the spectra which were analyzed. For objects which were observed more than once, we show the spectra from which we derived absorption line lists. Other spectra are available on our web site.

The absorption line lists, including identifications, are given electronically in Table 3, and on the web site.

## 2.4. Effect of Aperture Size on Line Detection and Measurement

Our dataset is a compilation of spectra taken in different apertures. Post-COSTAR the spectral line spread function (LSF) was similar for data taken in each aperture, and we neglected any differences. Pre-COSTAR, the LSF was significantly degraded and non-Gaussian for data taken in the A-1 (4.3") aperture (Smith & Hartig 1989; Evans 1993). The LSF in other apertures was similar to the post-COSTAR values.

Seventy-two of the objects in the sample were observed pre-COSTAR with A-1, and were not observed subsequently; these are listed in Table 4. In a few cases, however, observations were taken pre-COSTAR with A-1 and post-COSTAR or with a smaller aperture, with the same grating, so we could directly compare the line lists generated. For two objects, q1521+1009 and q1634+70437, we examined the G270H spectra in detail. For q1521+1009, 8 lines which were detected in the small aperture data were strong enough to have been expected to be detected above the  $5\sigma$  equivalent width threshold in the pre-COSTAR A-1 data; however only 6 were detected. For q1634+7037, the situation was worse: of the 57 strongest lines in the small aperture data should have been detected in the pre-COSTAR A-1 spectrum, but only 31 were.

Figure 2 shows the 4 spectra in question. The resolution is low in the pre-COSTAR A-1 spectra— 50% lower than in the small aperture data— and at  $z \sim 1$  our line search techniques apparently have not adequately taken into account the change in sensitivity.

While the spectra observed only in the A-1 aperture, pre-COSTAR are useful for some types of absorption line studies, we recommend that they *not* be used for studies of the Ly- $\alpha$  forest.

## 2.5. Comparison with the HST Quasar Absorption Line Key Project

A part of our sample contains absorption lines derived from the spectra observed for by the HST Key Project. We derived the absorption line properties independently from the Key Project for the same data, and in this section compare line lists. Although we reduced the spectral data slightly differently (weighting individual spectra by exposure time) the spectra for a few objects we checked are identical.

Figure 3 shows the comparison of the lines found by our software and the Key Project (J98). We chose 7 objects for detailed comparison (q0003+1553, q0743-6719, q1116+2135, q1241+1737, q1424-1150, q1718+4807, q2340-0339). These were chosen randomly from the objects which had reasonable signal to noise, contained Ly- $\alpha$  forest, did not have heavily

blended or broad absorption features, and appeared to have continua that should be fit easily. Of a total of 285 lines found by our software, 14 lines, or 5% of the total, were not found by the Key Project. In all cases, the features in question were weak, blended with other features, or near the edge of the spectrum.

Figure 3 shows the comparison of the equivalent widths and significance level for the lines which were detected in common by both groups. The significance level assigned to each line shows a systematic offset however. We assign a significance to the line which is about 20% lower than that assigned by the Key Project. As a result, our line lists are more conservative, and contain fewer lines above a given threshold. This difference is probably due to the fact that we adopt a fairly wide window (2.46 times the full-width-half-maximum of the spectral line spread function in pixels) in which to calculate the detection threshold, compared to J98.

These differences are larger than we expected. Since both groups have automated line finding and continuum fitting algorithms, the differences result from the slightly different approaches to line detection. The effects are easily quantifiable in subsequent analysis.

## 2.6. Completeness and Line Blending

In order to determine how reliably we find significant lines, we produced a set of 25  $z = 0.5$  simulated Ly- $\alpha$  forest spectra and a set of 25 spectra at  $z = 1$ . The code we used is described in Dobrzycki & Bechtold (1996). We modeled the Ly- $\alpha$  forest using the neutral hydrogen column density ( $N_{HI}$ ) and b-value distributions observed in high resolution optical spectra of high redshift quasars (Hu et al. 1995). We parameterized the number of lines  $N$  as

$$N \propto N_{HI}^{-\beta} \exp(-(b - \langle b \rangle)^2 / 2\sigma_b^2) (1 + z)^\gamma$$

and used values of  $\gamma = 0.50$  (Bahcall et al. 1993) and  $\beta = 1.46$  (Hu et al. 1995). The results of this analysis should not be sensitive to the value of  $\gamma$  since the redshift path covered in each spectrum is small. The lower column density limits chosen were  $5 \times 10^{12} \text{ cm}^{-2}$  for  $z = 0.5$  and  $2 \times 10^{12} \text{ cm}^{-2}$  for  $z = 1$ ; and the upper column density limit used was  $3 \times 10^{14} \text{ cm}^{-2}$  in both cases. The mean Doppler parameter and width of the Doppler parameter distribution used were  $\langle b \rangle = 28 \text{ km s}^{-1}$  and  $\sigma_b = 10 \text{ km s}^{-1}$ . The column density limits were chosen to give the same total absorption in the simulated spectra as is calculated in the spectra of q0850+4400 and q2145+0643, which served as the templates for the  $z = 0.5$  and  $z = 1$  simulations, respectively. We used the signal-to-noise, sampling, spectral resolution, and observed continuum of these two representative objects to model the Ly- $\alpha$  forest spectra.

We find that for the  $z = 0.5$  simulation, at  $5\sigma$  significance, the line lists are 100% complete; and for the  $z = 1$  simulation and  $5\sigma$  significance the line lists are 98% complete. In this calculation, we account for line blending by counting all simulated lines within 2.46 resolution elements of each recovered line as a component of that recovered line. If blending is neglected and matches are determined on the basis of the best wavelength match between simulated and recovered lines, the completenesses drop to 82% and 61% for  $z = 0.5$  and  $z = 1$  respectively. For lines of  $3\sigma$  significance and above, the completenesses of the  $z = 0.5$  and  $z = 1$  simulation line lists are 94% and 96% when blending is accounted for and 75% and 54% when it is not.

The simulations also revealed another interesting point. Of the lines “recovered” by our software, a small percentage were not generated by the simulation program. In other words, our software found some spurious lines. How many of these lines occur in the sample depends upon the signal-to-noise of the data and upon the line density of the spectra, i.e. the redshift. The percentages of these spurious lines were 5.3% of the  $3\sigma$  lines from the  $z = 0.5$  simulated spectra, and 1.3% of the  $3\sigma$  lines from the  $z = 1$  simulated spectra. The higher percentage of spurious lines in the  $z = 0.5$  spectra compared to the  $z = 1$  spectra, which have higher line densities, can be understood to be a result of the higher signal-to-noise in the  $z = 1$  simulated spectra. The signal-to-noise template for the  $z = 1$  simulations fluctuates between 12.5 and 14 across the spectra, while that of the  $z = 0.5$  simulations increases smoothly from 3 to 15 from the blue to the red. None of the lines recovered at  $5\sigma$  significance were spurious.

In summary, based on the analysis of simulated Ly- $\alpha$  forest spectra, we adopt  $3.5\sigma$  as the threshold for detection of real absorption lines, and  $5\sigma$  as the threshold for completeness.

### 3. Notes on Individual Quasars.

We discuss the individual quasars here. After each object, we specify G270( $n$ ), G190( $n$ ), G130( $n$ ), to indicate that  $n$  spectra taken with the G270H, G190H or G130H gratings were reduced. The emission line redshifts are taken from Hewitt & Burbidge (1993) or NED, unless otherwise noted.

q0002-4214,  $z = 2.76$ . This high redshift quasar has been the subject of several optical absorption line studies (Sargent et al. 1979, Boisse & Bergeron 1985). We identify several metal lines with previously known systems, at  $z = 2.46, 2.30, 2.16, 1.99,$  and  $1.54$ . G270.

q0002+0507,  $z = 1.90$ . UM18. This bright quasar has a well studied IUE spectrum, (Bechtold et al. 1984) and two previously known absorption line systems at  $z = 0.8514$  and  $z = 1.7444$  (Young, Sargent & Boksenberg 1982, Steidel & Sargent 1992). Churchill (1997)



reports a weak Mg II system at  $z = 0.5914$ . G270(2),G190.

q0003+0146,  $z = 0.234$ . G190.

q0003+1553,  $z = 0.450$ . PG. The continuum spectral energy distribution of this quasar is very well studied. J98 present the FOS spectrum. G270,G190,G130.

q0003+1955,  $z = 0.025$ . MRN 335. The absorption line spectrum was studied in detail by Stocke et al. (1995) and Shull, Stocke & Penton (1996), and four local absorbers were found. G270,G190,G130.

q0007+1041,  $z = 0.089$ . IIZw2. A well-studied low redshift Seyfert. A strong line at  $1322\text{\AA}$  may be associated Ly- $\alpha$ , with no corresponding metal-line absorption. G130,G270.

q0015+1612  $z = 0.553$ . The FOS spectrum is discussed in detail by Bechtold et al. (2001). G190.

q0017+0209,  $z = 0.401$ . Discovered in the LBQS survey (Foltz et al. 1989), the FOS spectrum is presented in Turnshek et al (1997) and J98. They argue convincingly that metal systems are detected at  $z = 0.5764$ ,  $1.3389$ , and  $1.3426$ , and less convincingly for several others. Churchill (1997) reports a Mg II system at  $z = 0.7289$  from optical spectra. We identified metal lines associated with these four systems. G190.

q0018+2825,  $z = 0.509$ . The object does not appear in NED. The redshift is determined from strong C IV and C III] emission lines at  $2342\text{\AA}$  and  $2886\text{\AA}$  respectively. A strong absorption line at  $2344\text{\AA}$  is probably associated C IV blended with interstellar Fe II  $\lambda 2344$ . G270.

q0024+2225,  $z = 1.108$ . The  $z = 1.11$  associated absorber described by Weymann et al. (1979) is confirmed. The FOS spectrum is referred to in Bahcall et al. (1993), and presented in J98. Other metal absorption line systems are reported by J98 at  $z = 0.8196$  and  $0.4069$ . G190, G270.

q0026+1259,  $z = 0.142$ . The continuum spectral energy distribution of this PG quasar has been studied extensively. G270, G190, G130(2).

q0042+1010,  $z = 0.583$ . Radio loud quasar with no previously published absorption line spectrum. A very strong line at  $1926\text{\AA}$  may be associated Ly- $\alpha$  and no obvious corresponding metal absorption. G270, G190.

q0043+0354,  $z = 0.384$ . The FOS spectra and the absorption line analysis are presented earlier in Turnshek et al. (1997) and Turnshek et al. (1994). Turnshek et al. (1997) describe the C IV absorber at  $z = 0.38$  as a “BAL” although it is very narrow and would be what

we call in this paper an “associated absorber”. Semantics aside, there is a strong absorption line system at the emission line redshift with Ly- $\alpha$  and C IV detected. G270, G190.

q0044+0303,  $z = 0.624$ . The FOS spectra are previously discussed in Bahcall et al. (1993). They describe C IV at  $z = 0.245$  and  $z = 0.449$ . The  $z = 0.449$  system may be identified with an intervening galaxy at the same redshift (Ellingson, Green & Yee 1991). The evidence for the  $z = 0.245$  spectrum is weak, given that only the C IV doublet is seen in the Ly- $\alpha$  forest part of the spectrum, so the probability of a chance coincidence is high. G270, G190.

q0050+1225,  $z = 0.061$ . IZw1. The discovery of very local Ly- $\alpha$  absorption in the spectrum is described by Shull, Stocke & Penton (1996) and Stocke et al (1995). Two systems, at  $z = 0.0538$  and  $0.05061$  appear to have Ly- $\alpha$  and metal line systems detected. G270(3), G190(2), G130.

q0052+2509,  $z = 0.155$ . G190.

q0058+0155,  $z = 1.954$ . PHL 938. We carried out an analysis of this spectrum, and identified a number of metal-line absorbers, at  $z = 0.612, 1.20, 1.26, \text{ and } 1.46$ . G190.

q0100+0205,  $z = 0.394$ . UM 301. G190(2).

q0102-2713,  $z = 0.780$ . This is an LBQS quasar (Morris et al. 1991), and has a strong intervening C IV absorber at  $z = 0.48$ . G190.

q0107-0235,  $z = 0.948$ . This is the brighter of the pair of LBQS quasars (Chaffee et al. 1991) whose FOS spectrum is discussed in detail by Dinshaw et al. (1995, 1997). G190.

q0107-0234,  $z = 0.942$ . This is the fainter of a pair of LBQS quasars (Chaffee et al. 1991) whose FOS spectrum is discussed in detail by Dinshaw et al. (1995, 1997). G190.

q0107-1537,  $z = 0.861$ . A strong C IV system is at  $z = 0.548$ . G270.

q0112-0142,  $z = 1.365$ . This is a well-studied Parkes radio-loud quasar, whose FOS spectrum was presented by Wills et al. (1992). We identify a candidate intervening damped Ly- $\alpha$  absorber at  $z = 1.19$ . G270.

q0115+0242,  $z = 0.672$ . PKS. G270, G190.

q0117+2118,  $z = 1.493$ . This well-studied PG quasar has optical absorption line spectra reported by Boisse et al. (1992), Steidel & Sargent (1992) and Rao, Turnshek & Briggs (1995). We identify lines from the  $z = 0.576, 1.047, 1.325$  and  $1.342$  discovered by these authors. There is a strong associated absorption complex at  $z = 1.447 - 1.506$ . G270(2), G190.

q0119-0437,  $z = 1.925$ . This high redshift quasar has a well-studied optical absorption line spectrum (Sargent, Boksenberg & Young 1982, Sargent, Steidel & Boksenberg 1988a). We identify lines associated with several intervening metal line absorption redshift systems. G270, G190.

q0121-5903,  $z = 0.047$ . Fairall 9. The Milky Way interstellar absorption is extremely strong, particularly the Si II 1260 line. G270, G190, G130.

q0122-0021,  $z = 1.070$ . The FOS spectra were discussed by Bergeron et al. (1994) and Bahcall et al. (1996). They identify intervening metal line absorbers at  $z = 0.398$  and  $z = 0.953$ . G270, G190.

q0125-0635,  $z = 0.005$ . This is the Sy 1, MRK 996. G190.

q0133+2042,  $z = 0.425$ . This is 3C47, whose FOS spectrum is described by Wills et al. (1995). There is a strong associated C IV absorber. G270, G190.

q0137+0116,  $z = 0.260$ . UM 355. This is a well-studied radio-loud quasar. G270, G190, G130.

q0143-0135,  $z = 3.124$ . UM 366. This is a high redshift quasar, detected to 581 Å in its rest frame. A damped Ly- $\alpha$  absorber is detected at  $z = 1.61$ , as well as lines from systems at  $z = 1.58$  and 1.28. G270.

q0150-2015,  $z = 2.139$ . This quasar has a well studied absorption line spectrum (Sargent, Steidel & Boksenberg 1988b, Steidel & Sargent 1992, Hamann 1997 and references therein), including a strong intrinsic absorber. G270, G190.

q0159-1147,  $z = 0.669$ . 3C57. The FOS spectra is described by Wills et al. (1992) and J98. A strong absorption line at the Ly- $\alpha$  emission line redshift (2028 Å) may be an associated metal-line absorber, although no associated Mg II absorption is reported by Aldcroft, Bechtold and Elvis (1994). The part of the FOS spectrum where C IV is expected coincides with strong lines of interstellar Fe II, and is inconclusive. Likewise several candidate metal absorbers are suggested by J98 but none are secure. G270, G190.

q0207-3953,  $z = 2.813$ . This is a well-studied high-redshift quasar, with a strong Lyman-limit at 3190 Å, which is 836 Å in its rest frame. G270.

q0214+1050,  $z = 0.408$ . PKS. This is a radio loud quasar, with no previous absorption line spectrum published. G270, G190.

q0219+4248,  $z = 0.444$ . 3C 66A. This is a BL Lac object. A number of weak absorption lines are seen, but none more significant than  $5\sigma$ . No broad emission lines are seen. G270,

G190, G130.

q0232-0415,  $z = 1.450$ . This Parkes radio loud quasar has been the subject of numerous continuum and optical absorption line studies. The  $z = 1.425$  C IV absorber reported by York et al. (1991) is not confirmed, since a strong Ly- $\alpha$  line is not apparent. We tentatively identify a system at  $z = 1.355$ . J98 discuss the FOS spectrum, and also identify several possible metal absorbers, but none are convincing, since they rely on only two identified lines, in confused regions of the spectrum. G270.

q0253-0138,  $z = 0.879$ . This is an LBQS quasar (Chaffee et al. 1991) whose absorption line spectrum is not previously reported. Only one significant line is seen, identified with ISM Mg II  $\lambda 2793$  absorption. G270.

q0254-3327b,  $z = 1.915$ . The quasars q0254-3327 a,b and c have been the subject of numerous studies. G270.

q0254-3327c,  $z = 1.863$ . G270, G190.

q0302-2223,  $z = 1.40$ . There is a damped Ly- $\alpha$  absorber at  $z = 0.99$ . We identify lines associated with several other systems. G270.

q0333+3208,  $z = 1.258$ . This is a very well studied radio-loud quasar. We confirm the Mg II absorber at  $z = 0.953$  described by Steidel & Sargent (1992). G270.

q0334-3617,  $z = 1.100$ . This is an X-ray selected quasar (Maccacaro et al. 1991, Stocke et al. 1991a). The strong absorption line at 2557 Å near the Ly- $\alpha$  emission line does not appear to have any metal absorption in C IV associated with it. G270.

q0349-1438,  $z = 0.616$ . 3C95. The FOS spectrum is presented by Bahcall et al. (1993). One metal-line absorber is seen, with  $z = 0.3566$ . G270, G190.

q0350-0719,  $z = 0.962$ . This is an interesting radio-loud quasar with a broad associated absorption line. See Aldcroft, Bechtold & Elvis (1994) for optical spectra. G270.

q0355-4820,  $z = 1.005$ . The FOS spectrum is discussed by Hamann, Zuo & Tytler (1995). We identify a strong metal system at  $z = 0.987$ . G270(2).

q0403-1316,  $z = 0.571$ . The FOS spectrum of this well-studied Parkes radio quasar is presented by Wills et al. (1995). G270, G190.

q0405-1219,  $z = 0.574$ . This quasar was discovered by IRAS (Low et al. 1988) and has a strong Ly- $\alpha$ -Ly- $\beta$  pair at  $z = 0.6276$ . No metal transitions are seen associated with this system however. The FOS spectrum is discussed in detail by Bahcall et al. (1993), with an updated discussion of the metal absorbers in J98. One of the G130H spectra was obtained

in SPECTROPOLARIMETRY mode and was not reduced. G270, G190, G130(2).

q0414-0601,  $z = 0.781$ . 3C110. The FOS spectrum is presented by J98. They do not report any metal-line systems, but we find a fairly convincing one at  $z = 0.664$ . G270(2), G190(2).

q0420-0127,  $z = 0.915$ . PKS. This is a well-studied quasar, with an optical absorption line spectrum reported by Aldcroft, Bechtold & Elvis (1994). G270.

q0421+0157,  $z = 2.044$ . PKS. The optical absorption line spectrum of this high redshift quasar is discussed by Steidel & Sargent (1992). G270.

q0424-1309,  $z = 2.159$ . PKS 0424-13. This optical absorption line spectrum of this high redshift quasar is discussed by Steidel & Sargent (1992). G270.

q0439-4319,  $z = 0.593$ . PKS. A low redshift damped Ly- $\alpha$  absorber at  $z = 0.101$  is identified by Petijean et al. (1996), who present the FOS data. In addition, we find another metal absorber at  $z = 0.44$ . The FOS spectra are also discussed by J98. G270, G190.

q0450-2958,  $z = 0.286$ . This IRAS selected quasar (Low et al. 1988) has been the subject of several studies. A strong associated C IV absorption trough is seen. G190.

q0453-4220,  $z = 2.66$ . This is a well studied high redshift quasar, with an optically thick Lyman limit at 3120 Å. G270, G190.

q0454-2203,  $z = 0.534$ . PKS. This is a PKS object whose optical absorption line spectrum is discussed by Aldcroft, Bechtold & Elvis (1994). Metal absorbers are found at  $z = 0.474$  and  $0.482$ . G270(2), G190(2), G130.

q0454+0356,  $z = 1.345$ . PKS. In this well-studied Parkes object we identify lines associated with previously known redshift systems at  $z = 1.15, 1.06, 0.85$ . G270(2), G190.

q0506-6113,  $z = 1.093$ . This is a blazar with a strong associated metal absorber at  $z = 1.079$ . G270.

q0518-4549,  $z = 0.0351$ . PKS, Pictor A. This is a well-studied low-redshift radio galaxy. G270, G190, G130.

q0537-4406,  $z = 0.894$ . A well-known blazar and gamma ray source, classified as a BL Lac. Strong emission lines are seen. G270.

q0624+6907,  $z = 0.374$ . An extremely luminous object found in the Hamburg survey (Reimers et al. 1995). The FOS spectrum is discussed by J98. G270(2), G190(2), G130.

q0637-7513,  $z = 0.656$ . We identify metal absorption at  $z = 0.152$  and  $0.416$ . The

spectrum is also discussed in J98. G270, G190.

q0710+1151,  $z = 0.768$ . 3C 175. A radio-loud quasar whose optical absorption line spectrum is discussed by Aldcroft, Bechtold & Elvis (1994). The FOS spectrum is described by Wills et al. (1995). One intervening metal absorber is identified at  $z = 0.463$ . G270, G190.

q0740+3800,  $z = 1.063$ . 3C 186. A radio loud quasar whose FOS spectrum is presented by Wills et al. (1995). We identify lines of intervening metal line systems at  $z = 0.885$  and an associated absorber at  $z = 1.069$ . See also Aldcroft, Bechtold & Elvis (1994). G270.

q0742+3150,  $z = 0.462$ . PKS. Another radio loud quasar, with an associated C IV absorber. A low redshift Mg II system at  $z = 0.1917$  suggested by Boisse et al. (1992) is not confirmed by the FOS spectrum. The spectrum is also discussed by J98. G270, G190.

q0743-6719,  $z = 1.511$ . PKS. A bright radio-loud quasar. A number of C IV absorbers are detected. The spectrum is discussed by J98. The G190H and one of the G270H spectra were taken in SPECTROPOLARIMETRY mode and were not reduced G270(2), G190.

q0823-2220,  $z = 0.910$ . PKS. This is a BL Lac object, with redshift limit determined by the strong absorption line system at  $z = 0.910$  (Falomo 1990). No emission lines are seen in the FOS spectrum. G270.

q0827+2421,  $z = 0.939$ . B2. A strong absorption line system is seen at  $z = 0.52$  (Ulrich & Owen 1977). G270.

q0838+1323,  $z = 0.684$ . 3C 207. There is a strong associated C IV system at  $z = 0.68$ . G270, G190.

q0844+3456,  $z = 0.064$ . Ton 951. Well studied PG quasar. An associated absorber is seen. G270, G130.

q0848+1623,  $z = 1.936$ . This is a high redshift quasar with an optically thick Lyman limit, and several metal lines associated with previously known redshift systems. G270.

q0850+4400,  $z = 0.513$ . US 1857. The FOS spectra were presented by Bahcall et al. (1993). G270, G190.

q0851+2017,  $z = 0.306$ . OJ +287. This is a well-known BL Lac object. No emission lines were detected. Several interstellar absorption lines are apparent. It is discussed in J98. One of the G270H and the G190H spectra were SPECTROPOLARIMETRY, and were not reduced. G270(2), G190.

q0859-1403,  $z = 1.327$ . PKS FOS data were presented by Wills et al. (1995). Aldcroft,

Bechtold & Elvis (1994) present an optical absorption line spectrum. A Mg II system at  $z = 0.209$  proposed by Boisse et al. (1992) is not confirmed, with no Fe II lines detected at the expected wavelengths at that redshift. G270.

q0903+1658,  $z = 0.411$ . 3C 215. The FOS spectrum is presented by Wills et al. (1995). G270, G190.

q0906+4305,  $z = 0.670$ . 3C 216. The FOS spectrum is presented by Wills et al. (1995). G270, G190.

q0907-0920,  $z = 0.625$ . This quasar was observed twice with the FOS. The first observation failed, and we so we analyzed the second one. G270(2).

q0916+5118,  $z = 0.553$ . We identify metal absorption lines at  $z = 0.51$  and  $0.24$ . The spectrum is discussed by J98. The  $z = 0.24$  system is not identified by these authors. G270, G190.

q0923+3915,  $z = 0.699$ . B2. This is a radio loud quasar whose FOS spectrum is discussed by Wills et al. (1995). A strong Ly- $\alpha$  associated absorption line is seen, but there is no corresponding N V. Only one of the G190H spectra were analyzed, since the other spectra had no signal. G270(2), G190(2).

q0933+7315,  $z = 2.528$ . This high redshift quasar has a strong Lyman limit system at  $3020 \text{ \AA}$ , and a well studied optical absorption line spectrum. Most of the lines in the FOS spectrum are associated with previously known metal absorption line redshift systems. G270.

q0935+4141,  $z = 1.97$ . PG. This bright PG quasar has been the subject of numerous studies. A damped Ly- $\alpha$  absorption line system is seen at  $z = 1.396$ . There is also a Lyman limit absorber at  $z = 1.4649$ . G270(2).

q0945+4053,  $z = 1.252$ . 4C+40.24. G270.

q0947+3940,  $z = 0.206$ . PG. A bright PG quasar with mostly ISM lines. G270, G190, G130.

q0953+4129,  $z = 0.239$ . PG. The FOS spectrum is discussed by J98. There is a strong Ly- $\alpha$  associated absorption line with no corresponding C IV absorption detected. G270, G190, G130.

q0953+5454,  $z = 2.584$ . This high redshift quasar has an optically thick Lyman limit at  $3230 \text{ \AA}$ . G270.

q0954+5537,  $z = 0.909$ . 4C+55.17. The FOS spectrum is presented by Wills et al.

(1995). G270, G190.

q0955+3238,  $z = 0.533$ . 3C 232. The optical absorption line spectrum of this object is well studied because of its chance projected proximity on the sky to a nearby galaxy (Stoche et al. 1991b and references therein.) Several lines associated with the foreground galaxy are detected, as well as an associated CIV absorber. The FOS spectrum is discussed by J98. G270, G190, G130.

q0957+5608A,  $z = 1.414$ . This is the well-known lensed quasar, with FOS spectra of both A and B images. There is a strong damped Ly- $\alpha$  system. The FOS spectra of both objects are discussed by Michalitsianos et al. (1997). G270.

q0957+5608B,  $z = 1.414$ . See notes for q0957+5608A. G270, G190.

q0958+2901,  $z = 0.1848$ . 3C 234. This object has narrow emission lines and what is probably an associated CIV absorber, although confirmation would require a spectrum which extends farther into the UV. G270, G190.

q0958+5509,  $z = 1.75$ . MRK 132. A well-studied high-redshift quasar with numerous lines from previously known metal absorption line systems detected. An optically thick Lyman limit cuts off the spectrum at 2500 Å. The spectrum presented here is somewhat higher signal-to-noise than the one presented in J98 for reasons which are not clear. G270.

q0959+6827,  $z = 0.773$ . G270, G190.

q1001+0527,  $z = 0.161$ . PG. The well studied quasar has a C IV absorption trough, at 1762 Å, near the emission line redshift. G270(2), G190(2), G130(2).

q1001+2239,  $z = 0.974$ . PKS. A radio loud quasar, with no previously published absorption line spectra. There are a few strong lines near the Ly- $\alpha$  emission line which don't appear to have metal absorption associated with them. G270.

q1001+291,  $z = 0.329$ . Ton 28. The FOS spectrum is presented by Bahcall et al. (1993). A broad absorption feature is seen at C III]  $\lambda 1909$  in the quasar rest frame. G270, G190, G130.

q1007+4147,  $z = 0.611$ . 4C 41.21 The optical absorption line spectrum is reported by Aldcroft, Bechtold & Elvis (1994). There is a metal absorption system at  $z = 0.389$ . G270, G190.

q1008+1319,  $z = 1.287$ . PG The optical absorption line spectrum is reported by Boisse et al. (1992), who detect Mg II systems at  $z = 1.159$  and 1.254. We detect a system at  $z = 0.90$ . G270.



q1010+3606,  $z = 0.070$ . CSO 251, Ton 1187. A low redshift Sy 1 galaxy. Strong absorption lines are seen at  $z \sim 0$ . G130.

q1017+2759,  $z = 1.928$ . Ton 34. A high redshift quasar, with known absorbers at several redshifts. The FOS spectrum is discussed in J98. G270.

q1026-0045a,  $z = 1.437$ . This is a bright LBQS quasar (Hewett, Foltz & Chaffee 1995). There is a strong metal absorber at  $z = 1.2959$ . There is a strong absorption line near emission Ly- $\alpha$  which does not appear to have any metal lines associated with it. G270.

q1026-0045b,  $z = 1.53$ . This is a bright LBQS quasar (Hewett, Foltz & Chaffee 1995). G270.

q1028+3118,  $z = 0.1782$ . B2 We identify a possible low redshift Mg II absorber at  $z = 0.0570$ . G270, G190(2).

q1038+0625,  $z = 1.270$  4C 06.41. We identify a metal absorber at  $z = 1.2449$ . There is also a previously known system at  $z = 0.441$ . There are a number of other possible metal absorber candidates described by J98, but they are not likely real. G270.

q1047+5503,  $z = 2.165$ . We identify several candidate metal absorbers, but most of the spectrum is blueward of Ly- $\beta$  in the quasar rest frame. G270.

q1049-0035,  $z = 0.357$ . PG There are strong associated absorbers at  $z = 0.3413$  and  $z = 0.34877$ . The  $z = 0.341$  system is discussed by J98. G270, G190.

q1055+2007,  $z = 1.110$ . PKS. There is a Lyman limit system reported for this object and we see Ly- $\alpha$  at  $z = 1.0373$  (J98). G270.

q1100-2629,  $z = 2.145$ . This high redshift quasar has numerous absorbers identified in optical spectra, but since the Ly- $\beta$  in the rest frame is at  $3226 \text{ \AA}$ , we did not attempt identifications. G270.

q1100+7715,  $z = 0.311$ . 3C249.1. This has an associated absorber at  $z = 0.308$ , seen in Ly- $\alpha$  and O VI, although J98 do not identify it as such. G270, G190.

q1103-0036,  $z = 0.425$ . PKS. This is a radio source and a PG quasar. The FOS spectra are presented by Wills et al. (1995). G270, G190.

q1103+6416,  $z = 2.19$ . This bright high redshift quasar was discovered by Reimers et al. (1995). There is an optically thick Lyman limit at  $2648 \text{ \AA}$ , probably the strong metal absorber at  $z = 1.891$ . G270, G190.

q1104-1805a,  $z = 2.303$ . This is a lensed quasar (Smette et al. 1995), and there are

several prominent metal absorbers but we did not attempt identifications since  $\text{Ly-}\beta$  in the quasar rest frame is redward of the FOS spectra. G270.

q1104-1805b,  $z = 2.303$ . See notes for q1104-1805a. G270.

q1104+1644,  $z = 0.634$ . We identify metal absorbers at  $z = 0.454$  and a tentative system at  $z = 0.387$ . G270, G190.

q1111+4053,  $z = 0.734$ . 3C 254. There is a strong associated absorber detected in O VI and N V. The FOS spectrum is shown by Wills et al. (1995). G270, G190.

q1114+4429,  $z = 0.144$ . PG. A strong associated absorber is seen. G270(2), G190(2), G130(2).

q1115+0802A1,  $z = 1.722$ . PG Lensed quasar. In addition to an absorber with  $z = 1.69$  near the quasar redshift, we find candidate metal absorbers with  $z = 1.04$  and  $0.99$ . G270(2).

q1115+0802A2,  $z = 1.722$ . PG. See discussion of q1115+0802a1. We identify candidate metal absorbers with  $z = 1.04$  and  $0.99$  in this image as well. G270(2).

q1115+4042,  $z = 0.154$ . PG. We identify a C IV system at  $z = 0.155$ . Most of the detected lines are from the ISM. G270, G190 G130.

q1116+2135,  $z = 0.117$ . PG. J98. G270(2), G190(2), G130.

q1118+1252,  $z = 0.685$ . This object has a strong associated metal-line absorber. G270, G190.

q1121+4218,  $z = 0.234$ . G190.

q1122-1648,  $z = 2.40$ . HE. We identify a  $z = 0.68$  metal absorption line system, described by Reimers et al. (1995). G270, G190.

q1124+2711,  $z = 0.378$ . This quasar is close in projection to the galaxy cluster Abell 1267, at  $v=9623$  km/sec. The C III]  $\lambda 1909$  profile is peculiar, but the features cannot be readily identified with absorption from the foreground Abell 1267 or other galaxies at  $z = 0.0529$  which are also nearby in the sky. G270.

q1127-1432,  $z = 1.187$ . PKS. The G190H spectrum had no signal and we did not process it. In the G270H spectrum, we identify lines with a  $z = 0.313$  reported by Bergeron & Boisse (1991). A system with  $z = 0.382$  also described by them would have no lines expected in the wavelength range covered. There is a strong associated Ly- $\alpha$  line but no detected metal absorption corresponding to it. G270.

q1130+1108,  $z = 0.510$ . J98. There is a strong associated absorber. G270, G190.

q1132-0302,  $z = 0.237$ . G190.

q1136-1334,  $z = 0.557$ . J98. We identify a C IV system at  $z = 0.332$ , which is not identified by J98. We do not identify a system they suggest, at  $z = 0.4064$ . G270, G190.

q1137+6604,  $z = 0.652$ . 3C263.0. There is previously reported associated absorption for this object by Aldcroft, Bechtold & Elvis (1994). A low redshift metal absorber is seen at  $z = 0.116$ . The FOS spectrum is discussed by Bahcall et al. (1993). G270(2), G190(2).

q1138+0204,  $z = 0.383$ . A strong associated absorber is seen. G190.

q1144-0115,  $z = 0.382$ . A noisy spectrum, with a C IV absorber seen at  $z = 0.37$ . G190.

q1146+1106c,  $z = 1.01$ . See discussion of q1146+103b. A probable metal absorption line system is seen at  $z = 0.85982$ , as well as associated O VI absorption at  $z = 1.01$ . The continuum shows a broad feature in the UV of uncertain origin. G190.

q1146+1103e,  $z = 1.10$ . See notes for q1146+1103b. There is a possible metal absorber at  $z = 0.79466$ . G190.

q1146+1104b,  $z = 1.01$ . This is a member of a group of quasars, within a few arcminutes of each other on the sky. While it has been suggested in the literature that these objects are lensed images of the same quasar, it's clear from the FOS spectra that this is not the case. G190.

q1146+1105d,  $z = 2.12$ . There was no flux in this spectrum and we did not analyze it. It is part of the group described in the notes for q1146+1103b.

q1148+5454,  $z = 0.978$ . G270(2), G190(2), G130.

q1150+4947,  $z = 0.334$ . G270, G190.

q1156+2123,  $z = 0.349$ . G270, G190.

q1156+2931,  $z = 0.729$ . 4C29.45. There is a strong associated absorber at  $z = 0.729$ . G270, G190.

q1156+6311,  $z = 0.594$ . This spectrum does not contain Ly- $\alpha$  and we did not analyze the absorption lines. G270.

q1202+2810,  $z = 0.165$ . GQ Comae. This is the well-known variable quasar. The FOS spectra are presented by J98. G270(2), G190(2), G130.

q1206+4557,  $z = 1.158$ . PG. J98 presented the FOS spectra. Metal absorption is seen at  $z = 0.927$ . G270, G190.

q1211+1419,  $z = 0.085$ . PG. Well-studied PG quasar. G270(2), G190(2), G130.

q1214+1804,  $z = 0.375$ . Probable associated absorption at  $z = 0.3684$ . Another strong Ly- $\alpha$  line at slightly higher redshift has no corresponding C IV absorption. G190.

q1215+6423,  $z = 1.288$ . 4C 64.15. There is a metal absorber at  $z = 0.99544$ . A complex of absorption at the Ly- $\alpha$  emission line could be associated Ly- $\alpha$  with no obvious metal absorption or a complex of C IV absorbers at  $z = 0.805$  and  $z = 0.810$ . G270.

q1216+0655,  $z = 0.334$ . J98 suggest a metal line absorber at  $z = 0.1247$  but there are not strong arguments supporting it. G270, G190, G130.

q1216+5032a,  $z = 1.450$ . This object and q1216+5032b are a pair of quasars separated by 9 " (Hagen et al. 1996). We identify a metal absorber at  $z = 0.98$ . G270.

q1219+0447,  $z = 0.094$ . There are metal absorption systems at  $z = 0.005$  and  $0.092$ . On the sky, the quasar is close to the foreground galaxy, M61. The FOS spectrum and the relation of the absorbers to M61 are discussed by Bowen, Blades & Pettini (1996). G270, G130.

q1219+7535,  $z = 0.070$ . MRK 205. The FOS spectra are presented by Bahcall et al. (1992) and J98, who discuss Mg II absorption associated with the foreground galaxy NGC 4319 at  $z = 0.0047$ . G270, G190, G130.

q1220+1601,  $z = 0.081$ . This AGN was discovered by Margon, Downes & Channan (1985). G270.

q1222+2251,  $z = 2.046$ . PG, TON 1530. The FOS spectra of this well-studied quasar are previously discussed by Impey et al. (1996). We identified lines associated with absorption line systems at  $z = 0.6681$ ,  $1.4867$ ,  $1.5239$ ,  $1.9372$ ,  $1.9805$ , and  $2.0555$ . The G270H and one of the G190H spectra are SPECTROPOLARIMETRY and were not reduced. G270, G190(2).

q1224-1116,  $z = 1.979$ . No signal was detected and so we did not process it.

q1225+3145,  $z = 2.219$ . B2. The FOS data for this well-studied quasar are described by Stengler-Larrea et al. (1995), and a ground-based echelle spectrum is given by Khare et al. (1997). We identify Ly- $\alpha$  and other transitions in systems at  $z = 1.227$  and  $1.429$  suggested by Khare et al. (1997), but do not confirm their  $z = 0.365$  system. We identify lines associated with other well-established systems at  $z = 1.6257$ ,  $1.7953$ ,  $1.8871$ ,  $1.8974$ . G270.

q1226p0219,  $z = 0.158$ . 3C 273. The FOS data are discussed in Bahcall et al. (1991).

3C273 was observed in SPECTROPOLARIMETRY mode also, but we did not analyze those data. G270, G130.

q1229-0207,  $z = 1.045$ . PKS. We identify lines associated with a damped Ly- $\alpha$  absorber at  $z = 0.395$  and two strong C IV systems at  $z = 0.756$  and  $z = 0.698$ . The FOS spectrum is discussed by Stocke et al. (1998). G270, G190.

q1230+0947,  $z = 0.420$ . LBQS. G190.

q1241+1737,  $z = 1.273$ . PG. J98 lists tentative metal absorbers at  $z = 1.272$ , 1.2154, and 0.9927. We identify lines of the system at  $z = 1.2154$  which is probably an associated absorber: strong O VI and Ly- $\alpha$  are present. G270.

q1247+2647,  $z = 2.043$ . PG. Well-studied quasar with a damped Ly- $\alpha$  absorber at  $z = 1.2276$ , first suggested by Lanzetta, Wolfe & Turnshek (1995) from IUE data. Optical absorption line spectra are presented by Sargent, Steidel & Boksenberg (1988b) and Steidel & Sargent (1992). We identify lines associated with absorbers at  $z = 1.22, 1.96$  and 1.41. G270(2).

q1248+3032,  $z = 1.061$ . B2. Well-studied radio-loud quasar with no previous absorption line spectra published. Several Ly- $\alpha$  lines are seen with no associated metal absorption. G270.

q1248+3142,  $z = 1.02$ . CSO173 Identified by Sanduleak & Pesch (1984), this object has no previous absorption line spectroscopy published. We find a fairly secure metal absorber at  $z = 0.6642$ , and two other tentative ones at  $z = 0.7323$  and 0.8961. G190.

q1248+4007,  $z = 1.030$ . PG. FOS data are presented by J98. We identify lines with redshift systems at  $z = 0.7760$  and 0.8553. G270, G190.

q1249+2929,  $z = 0.82$ . CSO176 Identified by Sanduleak & Pesch (1984), we identify absorbers with  $z = 0.4103, 0.5959, 0.70675$ . G190.

q1250+3122,  $z = 0.78$ . CSO179 Identified by Sanduleak & Pesch (1984), we identify absorbers with  $z = 0.5877, 0.6393, 0.6839$  and 0.72686. G190.

q1250+5650,  $z = 0.321$ . 3C277.1. The FOS spectrum is presented by Wills et al. (1995). G270, G190.

q1252+1157,  $z = 0.871$ . PKS. J98 list a metal absorber at  $z = 0.6395$ , which we adopt. G270, G190.

q1253-0531,  $z = 0.538$ . 3C279. One of the G190H spectra had no signal and was not reduced. G270, G190(2), G130.

q1257+3439,  $z = 1.375$ . B2. J98 report systems at  $z = 1.3799$  and  $1.0512$ , and we concur. G270.

q1258+2835,  $z = 1.355$ . A strong, broad associated Ly- $\alpha$  absorber is seen. G270.

q1259+5918,  $z = 0.472$ . PG. Bahcall et al. (1993) present the FOS spectrum. We identify lines with a system at  $z = 0.2196$ . G270, G190, G130.

q1302-1017,  $z = 0.286$ . PKS. J98 present the FOS spectrum. G270, G190, G130.

q1305+0658,  $z = 0.602$ . 3C281. J98 present the FOS spectrum. G270, G190.

q1306+3021,  $z = 0.806$ . J98 present the FOS spectrum. G270.

q1307+0835,  $z = 0.155$ . G190.

q1307+4617,  $z = 2.129$ . J98 present the FOS spectrum. We found metal absorption lines from systems at  $z = 2.08$ ,  $1.434$ , and  $1.306$ . G270, G190.

q1309+3531,  $z = 0.184$ . PG. A very strong damped Ly- $\alpha$  is seen near the emission redshift, at  $z = 0.17925$ . G270, G190, G130.

q1311+0217,  $z = 0.306$ . G190.

q1317-0142,  $z = 0.225$ . G190.

q1317+2743,  $z = 1.022$ . TON153. J98 present the FOS spectrum. G270, G190.

q1317+5203,  $z = 1.055$ . A broad associated absorber at  $z = 0.92895$  is seen. G270.

q1318+2903,  $z = 0.549$ . TON156. G270, G190.

q1318+2903a,  $z = 1.703$ . TON155. We find metal absorption at  $z = 1.139$ . G190.

q1320+2925,  $z = 0.960$ . TON157. G270, G190.

q1321+0552,  $z = 0.2051$ . G190.

q1322+6557,  $z = 0.168$ . PG. G270, G190, G130.

q1323+6530,  $z = 1.618$ . 4C65.15. There is a damped Ly- $\alpha$  absorber at  $z = 1.6101$ . G270.

q1327-2040,  $z = 1.169$ . PKS. A possible associated absorber is detected at Ly- $\alpha$ . G270.

q1328+3045,  $z = 0.849$ . 3C286.0 There is a damped Ly- $\alpha$  at  $z = 0.690$ . G270, G190.

q1329+4117,  $z = 1.93$ . PG. Damped Ly- $\alpha$  at  $z = 0.5193$ , and possibly  $z = 1.282$  are seen. G270, G190.

q1333+1740,  $z = 0.554$ . PG. J98 observed this quasar. G270, G190.

q1334-0033,  $z = 2.783$ . G270, G190.

q1334+2438,  $z = 0.1076$ . G270, G190.

q1338+4138,  $z = 1.219$ . Observed by J98. One of the G190H spectra was SPECTROPOLARIMETRY and was not reduced. G270, G190(2).

q1340-0038,  $z = 0.326$ . We find a metal line system at  $z = 0.2267$ . G190.

q1340+6036,  $z = 0.961$ . 3C288-1 There is a strong associated absorber. G270.

q1346+2637,  $z = 0.598$ . G270.

q1351+3153,  $z = 1.326$ . B2. There is a damped Ly- $\alpha$  at  $z = 1.1486$ , and a somewhat doubtful system at  $z = 1.1486$ . G270.

q1351+6400,  $z = 0.088$ . PG. A strong associated absorber is at  $z = 0.0820$ . G270, G190, G130.

q1352+0106,  $z = 1.117$ . PG. G270,G190(2).

q1352+1819,  $z = 0.152$ . PG. G270, G190, G130.

q1354+1933,  $z = 0.719$ . PKS. J98 observed this object, and list a metal absorption line system at  $z = 0.4563$ . We do not confirm a previously reported system at  $z = 0.4306$ . G270(2), G190(2).

q1355-4138,  $z = 0.313$ . G190.

q1356+5806,  $z = 1.375$ . 4C58-29. G270.

q1401+0952,  $z = 0.441$ . G190.

q1402+2609,  $z = 0.164$ . PG. G270, G190(3), G130.

q1404+2238,  $z = 0.098$ . PG. There is an associated absorber at  $z = 0.0915$ . G270, G190, G130.

q1407+2632,  $z = 0.944$ . PG. J98 presented the FOS data and suggested several redshift systems. We concur with the ones at  $z = 0.6828$ ,  $0.5998$ , and  $0.9566$ . G270,G190.

q1415+4343,  $z = 0.002$ . SBS. There is an associated absorber. G190.

q1415+4509,  $z = 0.114$ . PG. G270(2), G190, G130.

q1416-1256,  $z = 0.129$ . PG. G190.

q1416+0642,  $z = 1.436$ . 3C298. This radio loud quasar has an associated absorber at  $z = 1.437$ . G270.

q1424-1150,  $z = 0.806$ . PKS. J98 report a metal absorber at  $z = 0.6553$ . A previously suggested system at  $z = 0.7465$  is not confirmed. G270, G190.

q1425+2003,  $z = 0.111$ . G190.

q1425+2645,  $z = 0.366$ . B2. There is associated absorption at  $z = 0.3605$  and  $0.3643$ . G270, G190.

q1427+4800,  $z = 0.221$ . PG. There appears to be a damped Ly- $\alpha$  absorber at  $z = 0.1206$ . G270, G190, G130.

q1435-0134,  $z = 1.310$ . G270.

q1435+6349,  $z = 2.068$ . S4. Discussed by J98. Of the several metal line systems reported in the literature, we find evidence for the ones at  $z = 1.4792$ ,  $1.5925$ ,  $1.9242$  and  $1.0682$ . G270.

q1440+3539,  $z = 0.077$ . MRK478 We see an associated absorber. G270, G190(2), G130.

q1444+4047,  $z = 0.267$ . PG. G270, G190(2), G130.

q1451-3735,  $z = 0.314$ . PKS. G190, G130.

q1503+6907,  $z = 0.318$ . B2. There is an associated absorber. G270.

q1512+3701,  $z = 0.371$ . B2. A previously reported  $z = 0.3574$  system is not confirmed. G270, G190.

q1517+2356,  $z = 1.903$ . LB9612. G270, G190.

q1517+2357,  $z = 1.834$ . LB9605. One of the G190H spectra had no signal and was not reduced. G270, G190(2).

q1521+1009,  $z = 1.324$ . PG. Some of the spectra were SPECTROPOLARIMETRY and were not reduced. G270(3), G190(2).

q1538+4745,  $z = 0.770$ . PG. J98 present the spectrum and suggest several metal line systems. We concur with the ones at  $z = 0.729$ ,  $0.7705$ ,  $0.514$ ,  $0.706$ , and  $0.408$ . G270, G190.

q1542+5408,  $z = 2.371$ . SBS. We find metal absorption at  $z = 1.41$ ,  $0.1558$  and  $0.72$ . G270, G190.

q1544+4855,  $z = 0.400$ . There is a previously reported system at  $z = 0.0749$ , and other



systems we identify at  $z = 0.222$  and  $0.187$ . There is a fairly uncertain system at  $z = 0.276$ . One of the G130H spectra had no signal and was not reduced. G190, G130(2).

q1545+2101,  $z = 0.264$ . 3C323-1. There is an associated absorber. G270, G190, G130.

q1555+3313,  $z = 0.942$ . B2. G270.

q1611+3420,  $z = 1.401$ . A strong associated absorption with metals is seen. G270.

q1612+2611,  $z = 0.131$ . G190.

q1615+3229,  $z = 1.681$ . 3C332. G270, G190, G130.

q1618+1743,  $z = 0.555$ . 3C334.0. G270(2), G190(2).

q1622+2352,  $z = 0.927$ . 3C336.0. Damped Ly- $\alpha$  is present at  $z = 0.6543$  and  $0.8908$ . We find metal absorption at  $z = 0.4718$  as well. G270, G190.

q1623+2653,  $z = 2.526$ . There is a damped Ly- $\alpha$  absorber at  $z = 1.0397$ . G270.

q1626+5529,  $z = 0.133$ . PG. There is a strong associated absorber. G270, G190, G130.

q1630+3744,  $z = 1.478$ . G270, G190.

q1631+3930,  $z = 1.023$ . There is an associated absorber at  $z = 1.021$ . G270.

q1634+7037,  $z = 1.337$ . PG. Previously discussed by J98. The G190H and one of the G270H spectra were SPECTROPOLARIMETRY and were not reduced. G270(2), G190.

q1637+5726,  $z = 0.745$ . G270, G190.

q1641+3954,  $z = 0.595$ . 3C345. Some of the data were SPECTROPOLARIMETRY and were not reduced. G270(2), G190(2).

q1656+0519,  $z = 0.887$ . PKS. G270.

q1700+6416,  $z = 2.722$ . The FOS spectrum is discussed by Vogel & Reimers (1995). The spectral coverage is of the extreme UV and so we did not make a line list for this object. G270, G190(2), G130.

q1704+6048,  $z = 0.371$ . 3C351.0. There is an associated absorber at  $z = 0.3646$ . There are many systems reported in the literature, but we find evidence for  $z = 0.2216$ ,  $0.3172$ , and  $0.3646$  only. G270, G190, G130.

q1715+5331,  $z = 1.940$ . PG. J98 list  $z = 1.6333$ . We do not confirm a previously reported system at  $z = 0.3672$ . G270.

q1717+4901,  $z = 0.025$ . ARP102B. The signal to noise was low in the G130H spectrum.

No metal identifications were attempted. G270, G190, G130.

q1718+4807,  $z = 1.084$ . PG. J98 lists systems at  $z = 0.8929$ , 1.0323, and 1.0872. We find absorbers at  $z = 1.0323$ , 1.0872, and 0.7012. G270(3), G190(2).

q1803+7827,  $z = 0.680$ . S5. G270, G190.

q1821+1042,  $z = 1.360$ . PKS. G190.

q1821+6419,  $z = 0.297$ . Associated absorber. G270, G190, G130.

q1845+7943,  $z = 0.0561$ . 3C390.3. Associated absorber at  $z = 0.0506$ . G270, G190, G130.

q1928+7351,  $z = 0.302$ . 4C73.18. G270(2), G190(2).

q2041-1054,  $z = 0.035$ . MRK509. There is a strong associated absorber. G270, G190, G130.

q2112+0555,  $z = 0.398$ . PG. G270, G190.

q2128-1220,  $z = 0.501$ . PKS. There is a damped Ly- $\alpha$  at  $z = 0.429$ , see J98. G270, G190.

q2135-1446,  $z = 0.200$ . PKS. There is an associated absorber at  $z = 0.200$ . G190, G130.

q2141+1730,  $z = 0.213$ . Associated absorber at  $z = 0.2108$ . G270, G190(2), G130(2).

q2145+0643,  $z = 0.999$ . PKS. There are several metal absorption systems listed in NED, but only  $z = 0.7905$ , 0.7897, 0.6557 and 0.8797 are confirmed. G270, G190.

q2155-3027,  $z = 0.116$ . PKS. Although a BL Lac, the redshift is well-determined from spectroscopy of the nebulosity of the host galaxy and host cluster of galaxies (Falomo, Pesce & Treves 1993). All of the spectra are SPECTROPOLARIMETRY, except one of the G130H spectra. G270, G190, G130(2).

q2201+3131,  $z = 0.297$ . B2. A previously reported system at  $z = 0.282$  is not confirmed. G270, G190, G130.

q2212-2959,  $z = 2.703$ . PKS. G270.

q2216-0350,  $z = 0.901$ . PKS. G270(3), G190(4).

q2223-0512,  $z = 1.404$ . 3C446. A previously reported system at  $z = 0.4925$  is not confirmed. G270.

q2230+1128,  $z = 1.037$ . CTA102. G270.

q2243-1222,  $z = 0.630$ . PKS. G270, G190.

q2251-1750,  $z = 0.068$ . We see an associated absorber at  $z = 0.06329$ . G270, G190, G130.

q2251+1120,  $z = 0.323$ . PKS. There is an associated absorber at  $z = 0.3256$ . A previously reported system at  $z = 0.2633$  is not confirmed. Some of the spectra are SPECTROPOLARIMETRY and were not reduced. G270(2), G190(2), G130(2).

q2251+1552,  $z = 0.859$ . 3C454.3. Of several metal systems previously reported, we confirm those at  $z = 0.1538$ ,  $0.3906$ , and  $0.8137$ . G270(3), G190(3).

q2300-6823,  $z = 0.512$ . PKS. G270, G190.

q2308+0951,  $z = 0.432$ . PG. A weak associated absorber at  $z = 0.434$  is seen. G270, G190, G130.

q2340-0339,  $z = 0.896$ . PKS. J98 list a number of candidate metal redshifts. We use those at  $z = 0.6841$ ,  $0.4621$ ,  $0.4212$ , and  $0.8238$ . One of the G270H spectra was not reduced because it had no signal. G270(3), G190.

q2344+0914,  $z = 0.672$ . PKS. J98 lists  $z = 0.1176$  and  $0.4368$  for metal systems; we used  $z = 0.4368$  only. G270, G190.

q2347-4342,  $z = 2.90$ . G270, G190.

q2349-0125,  $z = 0.174$ . G190.

q2352-3414,  $z = 0.706$ . PKS. Discussed in J98. G270, G190.

#### 4. Description of Data Products and Web Site.

In addition to the electronic version of the tables and figures published here, we have put other electronic files on web sites at the Steward Observatory, at the University of Arizona, and the High Energy group at the Center for Astrophysics, see

<http://lithops.as.arizona.edu/~jill/QuasarSpectra> or

<http://hea-www.harvard.edu/QEDT/QuasarSpectra>.

We put there the reduced spectra shown in Figure 1, as well as other spectra which we reduced but did not use to construct absorption line lists. Data are available as ascii lists, or fits files. We also put the line lists with identifications of metal absorption lines, and the equivalent width threshold for detection as a function of wavelength for each analyzed

spectrum. A detailed description of the data format is given on the web site.

## 5. Summary

We reduced and analyzed all absorption line spectra of quasars taken with the Faint Object Spectrograph on board the Hubble Space Telescope. We present line lists and identifications of absorption line spectra in 271 quasars. Our sample represents a significant increase over previous studies; for comparison, the extensive Key Project data set (J98), is comprised of spectra for 66 quasars. The data set presented here is useful for many studies, particularly those which benefit from a large number of independent sight-lines. We have several studies underway, including the study of associated metal-line absorption, analysis of the Milky Way ISM lines, and analysis of the proximity effect to derive the evolution of the UV background at low redshift. We have presented the absorption line data in a way which we hope will enable other workers to carry out additional studies.

We thank Buell Jannuzi for his encouragement and advice. This research has made use of the NASA/IPAC Extragalactic Database (NED) which is operated by the Jet Propulsion Laboratory, California Institute of Technology, under contract with NASA. This project was supported by STScI grant No. AR-05785.02-94A, and No. GO-066060195A. AD acknowledges support from NASA Contract No. NAS8-39073 (ASC).

## REFERENCES

- Aldcroft, T. L., Bechtold, J., & Elvis, M. 1994, *ApJS*, 93, 1
- Bahcall, J. N., Jannuzi, B. T., Schneider, D. P., Hartig, G. F., Bohlin, R., & Junkkarinen, V. 1991, *ApJ*, 377, L5
- Bahcall, J. N., et al. 1993, *ApJS*, 87, 1
- Bahcall, J. N., et al. 1996, *ApJ*, 457, 19
- Bechtold, J. 1994, *ApJS*, 91, 1
- Bechtold, J. et al. 1984, *ApJ*, 281, 76.
- Bechtold, J. et al. 2001, in preparation
- Bergeron, J. & Boisse, P. 1991, *A&A*, 243, 344.
- Bergeron, J. et al. 1994 *ApJ*, 436, 33

- Bohlin, R. C., Savage, B. D. & Drake, J. F. 1978, *ApJ*, 244, 132
- Boisse, P. & Bergeron, J. 1985, *A&A*, 145, 59.
- Boisse, P., Boulade, O., Kunth, D., Tytler, D., & Vigroux, L. 1992 *A&A*, 262, 401
- Bowen, D., Blades, J. C., & Pettini, M. 1996, *ApJ*, 472, L77
- Burstein, D., & Heiles, C. 1982, *AJ*, 87, 1165
- Cardelli, J. A., Clayton, G. C., Mathis, J. S. 1989, *ApJ*, 345, 245.
- Chaffee, F. H. et al. 1991 *AJ*, 102, 461.
- Churchill, C. 1997, Ph.D. thesis.
- Dinshaw, N. et al. 1995 *Nature*, 373, 223.
- Dinshaw, N. et al. 1997 *ApJ*, 491, 45.
- Dobrzycki, A. & Bechtold, J. 1996, *ApJ*, 457, 102.
- Dobrzycki, A. et al. 2001, *ApJ*, in press
- Ellingson, E., Green, R. F. & Yee, H.K.C. 1991 *ApJ*, 378, 476.
- Evans, I. N. 1993 FOS Instrument Science Report CAL/FOS-104.
- Falomo, R. 1990, *ApJ*, 353, 114.
- Falomo, R., Pesce, J., Treves, A. 1993, *ApJ*, 411, L63.
- Foltz, C. B. et al. 1989, *AJ*, 98, 1959
- Hagen, J.-J., Hopp, U., Engels, D., Reimers, D. 1996, *A&A*, 308, L25.
- Hamann, F. 1997 *ApJS*, 109, 279.
- Hamann, F., Zuo, L. & Tytler, D. 1995 *ApJ*, 444, L69
- Hewett, P. C., Foltz, C. B. & Chaffee, F. E. 1995, *AJ*, 109, 1498.
- Hewitt, A. & Burbidge, G. 1993, *ApJS*, 87, 451.
- Hu, E. M., Kim, T.-S., Cowie, L., Songaila, A., & Rauch, M. 1995, *AJ*, 110, 1526.
- Impey, C., Perry, C., Malkan, M., Webb, W. 1996 *ApJ*, 463, 473.
- Jannuzi, B. T. et al. 1996, *ApJ*, 470, L11.
- Jannuzi, B. T. et al. 1998, *ApJS*, 118, 1. (J98)
- Keyes, C. D. et al. 1995, *Faint Object Spectrograph Instrument Handbook*, version 6.0.
- Khare, P. et al. 1997 *MNRAS*, 285, 167.
- Lanzetta, K., Wolfe, A. & Turnshek, D. 1995 *ApJ*, 440, 435.

- Low, F.J., Cutri, R. M., Huchra, J. P., Kleinman, S. G. 1988, ApJ, 327 , L41
- Maccacaro, T. et al. 1991, ApJ, 374, 117
- Margon, B., Downes, R. & Chanan G. 1985, ApJS, 59, 23.
- Michalitsianos, A. G. et al. 1997, ApJ, 474, 598.
- Morita, M., Bechtold, J., Wilden, B. & Dobrzycki, A. 2001, ApJ, submitted.
- Morris, S. et al. 1991, AJ, 102, 1627.
- Morton, D. 1991, ApJS, 77, 119.
- Morton, D., York, D. & Jenkins, E. 1988, ApJS, 68, 449.
- Petitjean, P., Surdej, J., Smette, A., Shaver, P., Muecket, J., Remy, M. 1996 A&A, 313, L25.
- Rao, S. M., Turnshek, D. & Briggs, F. 1995 ApJ, 449, 488.
- Reimers, D. et al. 1995,  $\alpha$ 303, 449.
- Sanduleak, N. & Pesch, P. 1984 ApJS, 55, 517.
- Sargent, W. L. W., Young, P. J., Boksenberg, A., Carswell, R. F., & Whelan, J. A. J. 1979 ApJ, 230, 49.
- Sargent, W. L. W., Boksenberg, A. & Young, P. 1982 ApJ, 252, 54.
- Sargent, W. L. W., Steidel, C. & Boksenberg, A. 1988a ApJ, 334, 22.
- Sargent, W. L. W., Steidel, C. & Boksenberg, A. 1988b ApJS, 68, 539.
- Schneider, D. P., et al. 1993, ApJS, 87, 45
- Scott, J., Bechtold, J., Dobrzycki, A. 2000a, ApJS, 130, 37. (Paper I)
- Scott, J., Bechtold, J., Dobrzycki, A., Kulkarni, V. 2000b, ApJS, 130, 67(Paper II)
- Scott, J. et al. 2001, ApJ, submitted.
- Shull, J.M., Stocke, J. T. & Penton, S. 1996 AJ, 111, 72
- Smette, A., Robertson, J., Shaver, R. A., Reimers, D., Wisotzki, L, Koehler, T. 1995, A&AS, 113, 199.
- Smith, T. Ed & Hartig, G. 1989 FOS Instrument Science Report CAL/FOS -061
- Stark, A. A., Gammie, C. F., Wilson, R. W., Bally, J., Linke, R. A.; Heiles, C., & Hurwitz, M. 1992, ApJS, 79, 77
- Steidel, C. & Sargent, W. L. W. 1992, ApJS, 80, 1
- Stengler-Larrea, E. et al. 1995 ApJ, 444, 64.
- Stocke, J. T. et al. 1991a ApJS, 76, 813.

- Stocke, J. T., Case, J., Donahue, M., Shull, J. & Snow, T. 1991b, *ApJ*, 374, 72.
- Stocke, J. T., Shull, J. M., Penton, S., Donahue, M. Carilli, C. 1995 *ApJ*, 451, 24.
- Stocke, J. T., Penton, S., Harvanek, M. & Neely, W. 1998 *AJ*, 115, 451.
- Turnshek, D. A. et al. 1994, *ApJ*, 428, 93.
- Turnshek, D. A. et al. 1996, *ApJ*, 463, 110.
- Turnshek, D. A., Monier, E. M., Sirola, C. J., & Espey, B. 1997, *ApJ*, 476, 40.
- Ulrich, M.-H., & Owen, F. N. 1977, *Nature*, 269, 673.
- Vogel, S. & Reimers, D. 1995, *A&A*, 294, 377.
- Weymann, R. J., Williams, R. E., Peterson, B. M., Turnshek, D. A. 1979 *ApJ*, 234, 33.
- Wills, B. J. et al. 1992 *ApJ*, 398, 454.
- Wills, B. J. et al. 1995 *ApJ*, 447, 139.
- York, D. et al. 1991 *MNRAS*, 250, 24.
- Young, P., Sargent, W. L. W. & Boksenberg, A. 1982 *ApJ*, 252, 10

Table 1. Quasars observed with FOS and G130H, G190H or G270H Gratings

Name	Status <sup>a</sup>	RA (1950)	Dec (1950)	RA (2000)	Dec (2000)	<i>z</i>	Alternate Name
q0002-4214		00 02 15.30	-42 14 11.0	00 04 48.20	-41 57 28.0	2.760	0002-422
q0002+0507		00 02 46.40	+05 07 29.3	00 05 20.20	+05 24 11.2	1.900	UM18=q0002+051
q0003+0146		00 03 13.82	+01 46 20.4	00 05 47.55	+02 03 02.2	0.234	Q0003+0146
q0003+1553		00 03 25.14	+15 53 07.3	00 05 59.22	+16 09 49.1	0.450	0003+15
q0003+1955		00 03 45.30	+19 55 28.5	00 06 19.52	+20 12 10.3	0.025	MRK335
q0005-2345	ND	00 05 27.47	-23 45 59.6	00 08 00.30	-23 29 18.0	1.407	PKS0005-239
q0007+1041		00 07 56.74	+10 41 47.8	00 10 30.94	+10 58 29.0	0.089	IIIZW2
q0015+1612		00 15 56.66	+16 12 46.6	00 18 31.90	+16 29 26.0	0.553	QSO0015+162
q0017+0209		00 17 51.15	+02 09 46.8	00 20 25.06	+02 26 25.3	0.401	Q0017+0209
q0018+2825		00 18 01.17	+28 25 52.4	00 20 38.00	+28 42 31.0	0.509	QSO0020+287
q0024+2225		00 24 38.58	+02 25 23.4	00 27 15.40	+22 41 59.0	1.108	NAB0024+22
q0026+1259		00 26 38.13	+12 59 29.2	00 29 13.71	+13 16 03.8	0.142	PG0026+12
q0031-7042	ND	00 31 58.81	-70 42 23.6	00 34 05.30	-70 25 52.0	0.363	MC40031-707
q0038+3242	ND	00 08 02.36	+32 42 05.7	00 40 43.50	+32 58 33.0	0.197	Q0038+327
q0042+1010		00 42 02.79	+10 10 28.9	00 44 58.78	+10 26 52.8	0.583	MC0042+101
q0043+0354		00 03 12.60	+03 54 00.8	00 45 47.20	+04 10 24.0	0.384	PG0043+039
q0044+0303		00 04 31.47	+03 03 32.8	00 47 05.90	+03 19 54.9	0.624	PKS0044+030
q0050-2523	ND	00 50 18.04	-25 23 09.1	00 52 44.70	-25 06 52.3	2.159	Q0050-253
q0050+1225		00 50 57.97	+12 25 20.2	00 53 35.02	+12 41 36.3	0.061	IZW1
q0052+2509		00 52 11.14	+25 09 24.5	00 54 52.13	+25 25 39.3	0.155	0052+2509
q0053-0119	ND	00 53 33.67	-01 19 53.7	00 56 07.10	-01 03 40.0	0.170	QSO0056-010
q0058+0155		00 58 19.72	+01 55 28.4	01 00 54.10	+02 11 37.0	1.954	PHL938
q0059-2735	ND	00 59 52.47	-27 35 56.6	01 02 17.01	-27 19 50.0	1.595	Q0059-2735
q0100+0205		01 00 38.61	+02 05 04.7	01 03 12.99	+02 21 10.4	0.394	0100+0205
q0102-2713		01 02 16.59	-27 13 12.2	01 04 41.00	-26 57 08.0	0.780	CT336
q0103-2622	ND	01 03 34.43	-26 22 23.7	01 05 59.00	-26 06 21.0	0.776	Q0103-2622
q0107-1537		01 07 03.18	-15 37 50.2	01 09 31.50	-15 21 52.0	0.861	QSO0107-156
q0107-0235		01 07 40.32	-02 35 51.0	01 10 13.15	-02 19 54.0	0.948	Q0107-025A
q0107-0234		01 07 43.48	-02 34 49.7	01 10 16.32	-02 18 52.8	0.942	Q0107-025B
q0110+2942	ND	01 10 38.68	+29 42 22.9	01 13 24.21	+29 58 15.8	0.363	B20110+29
q0112-0142		01 12 44.02	-01 42 55.1	01 15 17.12	-01 27 04.9	1.365	PKS0112-017
q0113+3249	ND	01 13 19.72	+32 49 32.4	01 16 07.28	+33 05 21.6	0.016	MRK1
q0115+0242		01 15 43.68	+02 42 19.9	01 18 18.46	+02 58 05.9	0.672	0115+027
q0117+2118		01 17 34.69	+21 18 02.7	01 20 17.30	+21 33 46.0	1.493	PG0117+213
q0119-0437		01 19 55.96	-04 37 08.1	01 22 27.90	-04 21 28.0	1.925	PKS0119-04
q0121-5903		01 21 51.24	-59 03 59.1	01 23 45.72	-58 48 21.8	0.047	FAIRALL9
q0122-0021		01 22 55.31	-00 21 31.6	01 25 28.90	-00 05 56.5	1.070	PKS0122-003
q0125-0635		01 25 04.56	-06 35 07.7	01 27 35.47	-06 19 35.9	0.005	SBS0125-065
q0133+2042		01 33 40.54	+20 42 09.4	01 36 24.47	+20 57 26.5	0.425	3C47-0
q0137+0116		01 37 22.90	+01 16 35.7	01 39 57.27	+01 31 46.3	0.260	PHL1093
q0143-0135		01 43 18.20	-01 35 30.8	01 45 51.20	-01 20 31.0	3.124	UM366
q0150-2015		01 50 05.04	-20 15 53.4	01 52 27.29	-20 01 07.2	2.139	UM675
q0151+0433	ND	01 51 51.70	+04 33 35.6	01 54 27.98	+04 48 17.9	0.404	0151+0433
q0159-1147		01 59 30.45	-11 47 00.0	02 01 57.20	-11 32 33.7	0.669	3C57
q0200-0858	ND	02 00 57.78	-08 58 11.2	02 03 26.18	-08 43 48.3	0.770	0200-0858
q0207-3953		02 07 24.42	-39 53 49.2	02 09 28.60	-39 39 40.0	2.813	Q0207-398
q0214+1050		02 14 26.76	+10 50 18.4	02 17 07.67	+11 04 09.6	0.408	PKS0214+10
q0219+4248		02 19 30.06	+42 48 30.0	02 22 39.62	+43 02 08.1	0.444	3C66A



Table 1—Continued

Name	Status <sup>a</sup>	RA (1950)	Dec (1950)	RA (2000)	Dec (2000)	<i>z</i>	Alternate Name
q0226-1024	BAL	02 26 12.74	-10 24 32.0	02 28 39.15	-10 11 10.3	2.256	Q0226-104
q0232-0415		02 32 36.62	-04 15 10.6	02 35 07.30	-04 02 06.0	1.450	PKS0232-04
q0237-2322	ND	02 37 52.72	-23 22 08.7	02 40 08.10	-23 09 18.0	2.223	PKS0237-233
q0240+0044	ND	02 40 05.80	+00 44 18.9	02 42 40.12	+00 57 02.6	0.569	EX0240+007
q0253-0138		02 53 44.08	-01 38 41.2	02 56 16.52	-01 26 37.4	0.879	0253-0138
q0254-3327	ND	02 54 39.31	-33 27 27.0	02 56 42.49	-33 15 25.2	1.915	PKS0254-334
q0254-3327b		02 54 39.42	-33 27 24.4	02 56 42.60	-33 15 22.6	1.915	PKS0254-334
q0254-3327c	BAL	02 54 04.61	-03 27 29.0	02 56 47.78	-33 15 27.5	1.863	Q0254-334
q0256+3637	ND	02 56 49.93	+36 37 20.7	02 59 58.61	+36 49 14.1	0.012	MRK1066
q0302-2223		03 02 35.74	-22 23 29.3	03 04 49.80	-22 11 52.0	1.400	1E0302-223
q0311+4151	ND	03 11 42.86	+41 51 03.4	03 15 01.40	+42 02 09.4	0.024	MRK1073
q0318-1937	ND	03 18 05.56	-19 37 18.4	03 20 21.15	-19 26 31.7	0.104	0318-196
q0333+3208		03 03 02.53	+32 08 36.3	03 36 30.17	+32 18 29.0	1.258	NRAO140
q0334-3617		03 34 15.06	-36 17 25.1	03 36 09.28	-36 07 33.3	1.100	0334-3617
q0349-1438		03 49 09.56	-14 38 06.3	03 51 28.60	-14 29 09.1	0.616	3C95
q0350-0719		03 50 04.07	-07 19 05.6	03 52 30.56	-07 11 02.0	0.962	0350-0719
q0355-4820		03 55 52.53	-48 20 48.8	03 57 21.90	-48 12 15.0	1.005	0355-4820
q0403-1316		04 03 14.01	-13 16 18.4	04 05 33.98	-13 08 14.1	0.571	PKS0403-13
q0405-1219		04 05 27.49	-12 19 31.7	04 07 48.40	-12 11 36.0	0.574	PKS0405-12
q0414-0601		04 14 49.33	-06 01 05.0	04 17 16.75	-05 53 45.9	0.781	PKS0414-06=3C110
q0420-0127		04 20 43.54	-01 27 29.7	04 23 15.80	-01 20 34.0	0.915	PKS0420-01
q0421+0157		04 21 32.71	+01 57 32.7	04 24 08.60	+02 04 25.0	2.044	PKS0421+01
q0424-1309		04 24 47.72	-13 09 33.9	04 27 07.20	-13 02 54.0	2.159	PKS0424-13
q0439-4319		04 39 42.76	-43 19 24.4	04 41 17.30	-43 13 43.7	0.593	PKS0439-433
q0450-2958		04 50 33.03	-29 58 30.1	04 52 30.00	-29 53 35.0	0.286	IR0450-2958
q0453-4220		04 53 47.60	-42 20 59.0	04 55 23.00	-42 16 17.0	2.66	Q0453-423
q0454-2203		04 54 01.16	-22 03 49.4	04 56 08.90	-21 59 09.4	0.534	PKS0454-22
q0454+0356		04 54 09.02	+03 56 14.3	04 56 47.17	+04 00 52.7	1.345	PKS0454+039
q0506-6113		05 06 08.59	-61 13 32.1	05 06 44.10	-61 09 40.0	1.093	0506-6113
q0513-0012	ND	05 13 38.03	-00 12 15.1	05 16 11.51	-00 08 59.2	0.033	AKN120
q0518-4549		05 18 23.60	-45 49 43.0	05 19 49.60	-45 46 44.0	0.0351	PKS0518-45
q0537-4406		05 37 21.12	-44 06 44.8	05 38 50.36	-44 05 09.1	0.894	0537-4406
q0624+6907		06 24 35.31	+69 07 03.2	06 30 02.70	+69 05 04.0	0.374	HS0624+6907
q0637-7513		06 37 23.50	-75 13 37.3	06 35 46.70	-75 16 16.6	0.656	PKS0637-75
q0710+1151		07 10 15.41	+11 51 23.7	07 13 02.39	+11 46 15.5	0.768	3C175=0710+118
q0740+3800		07 40 56.82	+38 00 30.7	07 44 17.47	+37 53 16.9	1.063	3C186=0740+380
q0742+3150		07 42 30.83	+31 50 15.4	07 45 41.70	+31 42 55.7	0.462	B20742+318
q0743-6719		07 43 22.28	-67 19 07.9	07 43 31.70	-67 26 25.0	1.511	PKS0743-67
q0749+2550	ND	07 49 34.82	+25 50 25.4	07 52 37.05	+25 42 38.5	0.446	OI-287
q0823-2220		08 23 50.00	-22 20 34.6	08 26 01.50	-22 30 27.0	0.910	PKS0823-22
q0827+2421		08 27 54.40	+24 21 07.8	08 30 52.09	+24 10 59.9	0.935	B20827+24
q0830+1133	ND	08 30 29.96	+11 33 52.6	08 33 14.40	+11 23 36.0	2.976	MG0833+112
q0838+1323		08 38 01.75	+13 23 05.8	08 40 47.56	+13 12 23.7	0.684	3C207=0838+133
q0844+3456		08 44 33.99	+34 56 07.9	08 47 42.49	+34 45 03.5	0.064	TON951
q0848+1623		08 48 53.67	+16 23 40.0	08 51 41.80	+16 12 22.0	1.936	Q0848+163
q0850+4400		08 50 13.46	+44 00 24.0	08 53 34.20	+43 49 01.0	0.513	US1867=0850+440
q0851+2017		08 51 57.33	+20 17 57.9	08 54 48.89	+20 06 30.1	0.306	OJ287
q0859-1403		08 59 54.97	-14 03 39.2	09 02 16.80	-14 15 31.1	1.327	PKS0859-14

Table 1—Continued

Name	Status <sup>a</sup>	RA (1950)	Dec (1950)	RA (2000)	Dec (2000)	<i>z</i>	Alternate Name
q0903+1658		09 03 44.17	+16 58 16.4	09 06 31.86	+16 46 12.2	0.411	3C215=0903+169
q0903+1734	ND	09 03 50.00	+17 34 27.6	09 06 38.21	+17 22 23.1	2.771	H0903+175
q0906+4305		09 06 17.35	+43 05 59.6	09 09 33.53	+42 53 47.0	0.670	3C216-0
q0907-0920		09 07 04.52	-09 20 10.1	09 09 30.70	-09 32 24.0	0.625	QSO0909-095-HOPR
q0916+5118		09 16 30.10	+51 18 52.6	09 19 57.70	+51 06 10.0	0.553	NGC2841UB3=0916+513
q0923+3915		09 23 55.42	+39 15 23.7	09 27 03.05	+39 02 20.9	0.699	B20923+39
q0932+5006	ND	09 32 32.15	+50 06 39.6	09 35 53.13	+49 53 13.6	1.920	Q0932+501
q0933+7315		09 33 05.03	+73 15 27.2	09 37 48.80	+73 01 58.0	2.528	TB0933+733
q0935+4141		09 35 48.76	+41 41 55.5	09 38 57.00	+41 28 21.3	1.937	PG0935+416
q0940+5425	ND	09 40 51.06	+54 25 14.2	09 44 17.22	+54 11 27.0	0.006	SBS0940+544
q0945+4053		09 45 50.13	+40 53 43.9	09 48 55.33	+40 39 45.0	1.252	4C40-24
q0946+3009	ND	09 46 46.42	+30 09 20.0	09 49 41.11	+29 55 19.1	1.216	PG0946+301
q0947+3940		09 47 44.85	+39 40 54.4	09 50 48.40	+39 26 51.0	0.206	PG0947+396
q0953+4129		09 53 48.26	+41 29 40.4	09 56 52.40	+41 15 23.0	0.239	PG0953+414
q0953+5454		09 53 52.04	+54 54 34.9	09 57 14.70	+54 40 17.0	2.584	SBS0953+54
q0954+5537		09 54 14.39	+55 37 16.5	09 57 38.16	+55 22 57.7	0.909	4C55-17=0954+556
q0955+3238		09 55 25.52	+32 38 23.1	09 58 21.00	+32 24 02.2	0.533	3C232=0955+326
q0957+5608a		09 57 57.37	+56 08 22.1	10 01 20.74	+55 53 55.1	1.414	0957+561A
q0957+5608b		09 57 57.52	+56 08 16.2	10 01 20.89	+55 53 49.2	1.414	0957+561B
q0958+2901		09 58 57.36	+29 01 37.7	10 01 49.50	+28 47 09.0	0.185	3C234
q0958+5509		09 58 08.23	+55 09 06.4	10 01 29.80	+54 54 39.0	1.75	MARK132
q0959+6827		09 59 09.72	+68 27 47.8	10 03 06.80	+68 13 17.5	0.773	0959+68W1
q1001+0527		10 01 43.30	+05 27 34.5	10 04 20.10	+05 13 00.0	0.161	PG1001+054
q1001+2239		10 01 58.54	+22 39 54.1	10 04 45.74	+22 25 19.1	0.974	PKS1001+22
q1001+2910		10 01 10.73	+29 10 08.4	10 04 02.60	+28 55 35.0	0.329	TON28=1001+291
q1007+4147		10 07 26.12	+41 47 25.8	10 10 27.50	+41 32 39.1	0.611	4C41.21=1007+417
q1008+1319		10 08 29.87	+13 19 00.5	10 11 10.80	+13 04 12.0	1.287	PG1008+133
q1010+3606		10 10 07.39	+36 06 15.1	10 13 03.17	+35 51 23.1	0.070	CSO251
q1017+2759		10 17 07.82	+27 59 06.7	10 19 56.63	+27 44 01.3	1.928	TON34
q1026-0045a		10 26 01.66	-00 45 22.6	10 28 35.00	-01 00 44.0	1.437	Q1026-0045-A
q1026-0045b		10 26 03.65	-00 45 06.6	10 28 37.00	-01 00 28.0	1.53	Q1026-0045-B
q1028+3118		10 28 09.81	+31 18 21.1	10 30 59.10	+31 02 56.0	0.178	B21028+313
q1030+6017	ND	10 30 51.49	+60 17 21.9	10 34 08.57	+60 01 52.0	0.051	MARK34
q1038+0625		10 38 40.99	+06 25 58.6	10 41 17.20	+06 10 17.0	1.270	4C06.41
q1047+5503		10 47 43.15	+55 03 13.6	10 50 45.80	+54 47 19.0	2.165	FBS1047+550
q1049-0035		10 49 18.06	-00 35 21.7	10 51 51.50	-00 51 18.1	0.357	PG1049-005
q1055+2007		10 55 37.61	+20 07 05.1	10 58 17.90	+19 51 50.7	1.110	PKS1055+20
q1100-2629		11 00 59.93	-26 29 05.4	11 03 25.26	-26 45 15.7	2.145	Q1101-264
q1100+7715		11 00 27.51	+77 15 08.7	11 04 13.90	+76 58 58.2	0.311	3C249-1=1100+772
q1101+3828	ND	11 01 40.64	+38 28 42.8	11 04 27.32	+38 12 31.5	0.031	MRK421
q1103-0036		11 03 58.27	-00 36 39.8	11 06 31.75	-00 52 53.4	0.425	PKS1103-006
q1103+6416		11 03 04.08	+64 16 21.9	11 06 10.80	+64 00 09.0	2.19	HS-1103+6416
q1104-1805a		11 04 04.95	-18 05 10.1	11 06 33.50	-18 21 24.0	2.303	HE-1104-1805A
q1104-1805b		11 04 05.05	-18 05 12.1	11 06 33.60	-18 21 26.0	2.303	HE-1104-1805B
q1104+1644		11 04 36.66	+16 44 16.7	11 07 15.00	+16 28 02.4	0.634	MC1104+167
q1111+4053		11 11 53.35	+40 53 41.4	11 14 38.70	+40 37 20.1	0.734	3C254=1111+408
q1114+4429		11 14 20.00	+44 29 57.4	11 17 06.30	+44 13 34.0	0.144	PG1114+445
q1115+0802a1		11 15 41.52	+08 02 23.3	11 18 16.94	+07 45 58.9	1.722	PG1115+080A1

Table 1—Continued

Name	Status <sup>a</sup>	RA (1950)	Dec (1950)	RA (2000)	Dec (2000)	z	Alternate Name
q1115+0802a2		11 15 41.52	+08 02 23.3	11 18 16.94	+07 45 58.9	1.722	PG1115+080A2
q1115+4042		11 15 45.91	+40 42 19.6	11 18 30.30	+40 25 55.0	0.154	PG1115+407
q1116+2135		11 16 30.21	+21 35 43.1	11 19 08.70	+21 19 18.0	0.117	PG1116+215
q1118+1252		11 18 53.46	+12 52 43.8	11 21 29.76	+12 36 16.9	0.685	MC1118+12
q1120+0154	ND	11 20 46.67	+01 54 16.3	11 23 20.70	+01 37 48.0	1.465	UM425
q1121+4218		11 21 55.83	+42 18 14.4	11 24 39.17	+42 01 45.2	0.234	Q1121+423
q1122-1648		11 22 12.28	-16 48 48.4	11 24 42.80	-17 05 18.0	2.40	HE-1122-1649
q1123+3935	ND	11 23 45.98	+39 35 15.4	11 26 28.00	+39 18 45.0	1.470	B31123+395
q1124+2711		11 24 57.64	+27 11 21.3	11 27 36.40	+26 54 50.0	0.378	QSO1127+269
q1127-1432		11 27 35.71	-14 32 54.8	11 30 07.02	-14 49 27.6	1.187	PKS1127-14
q1129-0229	ND	11 29 56.55	-02 29 25.9	11 32 29.85	-02 46 00.0	0.333	Q1129-0229
q1130+1108		11 30 55.04	+11 08 57.7	11 33 30.30	+10 52 23.0	0.510	1130+106Y=1130+111
q1132-0302		11 32 31.64	-03 02 17.0	11 35 04.90	-03 18 52.5	0.237	Q1132-0302
q1136-1334		11 36 38.58	-13 34 05.7	11 39 10.70	-13 50 43.1	0.557	PKS1136-135
q1137+6604		11 37 09.44	+66 04 27.0	11 39 57.10	+65 47 49.4	0.652	3C263.0=1137+660
q1138+0204		11 38 47.83	+02 04 41.5	11 41 21.71	+01 48 03.3	0.383	Q1138+0204
q1144-0115		11 44 44.44	-01 15 27.5	11 47 18.03	-01 32 07.7	0.382	Q1144-0115=1144-012
q1144-3755	ND	11 44 30.88	-37 55 31.0	11 47 01.32	-38 12 11.1	1.048	1144-3755
q1146+1106c		11 46 04.93	+11 06 57.7	11 48 39.40	+10 50 17.0	1.01	1146+111C
q1146+1103e		11 46 07.54	+11 03 49.7	11 48 42.00	+10 47 09.0	1.10	1146+111E
q1146+1104b		11 46 09.84	+11 04 37.7	11 48 44.30	+10 47 57.0	1.01	1146+111B
q1146+1105d	ND	11 46 16.84	+11 05 04.7	11 48 51.30	+10 48 24.0	2.12	1146+111D
q1146+1111	ND	11 46 13.46	+11 11 39.1	11 48 47.86	+10 54 58.6	0.863	MC1146+111
q1148+5454		11 48 42.64	+54 54 13.9	11 51 20.44	+54 37 32.8	0.978	1148+5454
q1150+4947		11 50 48.06	+49 47 50.0	11 53 24.46	+49 31 08.6	0.334	LB2136
q1156+2123		11 56 52.30	+21 23 38.2	11 59 26.20	+21 06 56.2	0.349	TEX1156+213
q1156+2931		11 56 57.93	+29 31 25.6	11 59 31.90	+29 14 43.6	0.729	4C29.45=1156+295
q1156+6311		11 56 04.72	+63 11 10.0	11 58 39.91	+62 54 28.1	0.594	1156+6311
q1202+2810		12 02 09.05	+28 10 53.9	12 04 42.20	+27 54 12.0	0.165	PG1202+281
q1206+4557		12 06 26.62	+45 57 17.4	12 08 58.00	+45 40 36.0	1.158	PG1206+459
q1211+1419		12 11 44.95	+14 19 52.7	12 14 17.68	+14 03 12.3	0.085	PG1211+1431
q1213-0017	ND	12 13 16.01	-00 17 53.8	12 15 49.80	-00 34 34.0	2.69	UM485
q1214-2745	ND	12 14 40.91	-27 45 52.8	12 17 17.06	-28 02 32.4	0.026	T1214-277
q1214+1804		12 14 16.83	+18 04 44.2	12 16 49.05	+17 48 04.5	0.375	Q1214+1804
q1215+6423		12 15 17.13	+64 23 46.8	12 17 40.86	+64 07 07.4	1.288	4C64-15
q1216-0102	ND	12 16 09.13	-01 02 47.5	12 18 42.92	-01 19 26.6	0.415	1216-0103
q1216+0655		12 16 47.84	+06 55 17.3	12 19 20.90	+06 38 38.4	0.334	PG1216+069
q1216+5032a		12 16 13.49	+50 32 15.1	12 18 41.10	+50 15 36.0	1.450	HS-1216+5032A
q1216+5032b	ND	12 16 12.99	+50 32 23.1	12 18 40.60	+50 15 44.0	1.451	HS-1216+5032B
q1219+0447		12 19 04.73	+04 47 03.8	12 21 37.94	+04 30 25.7	0.094	1219+047
q1219+7535		12 19 33.51	+75 35 16.1	12 21 44.04	+75 18 38.1	0.070	1219+7535 MRK 205
q1220+1601		12 20 58.98	+16 01 45.2	12 23 30.82	+15 45 07.9	0.081	1220+1601
q1222+2251		12 22 56.65	+22 51 49.4	12 25 27.39	+22 35 13.0	2.046	PG1222+228
q1224-1116	ND	12 24 47.18	-11 16 58.9	12 27 22.40	-11 33 34.4	1.979	Q1224-1116
q1225+3145		12 25 56.10	+31 45 12.1	12 28 24.92	+31 28 37.1	2.219	B21225+317
q1226+0219		12 26 33.25	+02 19 43.46	12 29 06.70	+02 03 08.60	0.158	3C273
q1229-0207		12 29 25.96	-02 07 32.4	12 32 00.00	-02 24 05.4	1.045	PKS1229-02
q1229+6430	ND	12 29 16.13	+64 30 50.8	12 31 31.40	+64 14 17.6	0.170	1229+6430

Table 1—Continued

Name	Status <sup>a</sup>	RA (1950)	Dec (1950)	RA (2000)	Dec (2000)	<i>z</i>	Alternate Name
q1230+0947		12 30 53.69	+09 47 55.2	12 33 25.79	+09 31 23.0	0.420	1230+0947
q1241+1737		12 41 41.03	+17 37 28.5	12 44 10.80	+17 21 04.0	1.273	PG1241+176
q1244+3225	ND	12 44 55.48	+32 25 28.8	12 47 20.80	+32 09 07.0	0.949	B21244+32B
q1245+3431	ND	12 45 03.21	+34 31 30.7	12 47 27.80	+34 15 09.0	2.068	B19
q1246-0542	ND	12 46 38.73	-05 42 59.1	12 49 13.84	-05 59 19.3	2.236	1246-057
q1247+2647		12 47 39.14	+26 47 26.8	12 50 05.73	+26 31 07.5	2.043	PG1247+267
q1248+3032		12 48 00.21	+30 32 58.8	12 50 25.54	+30 16 39.8	1.061	B21248+30
q1248+3142		12 48 25.36	+31 42 11.6	12 50 50.30	+31 25 53.0	1.02	CSO173
q1248+4007		12 48 26.65	+40 07 58.2	12 50 48.30	+39 51 39.6	1.030	PG1248+401
q1249+2929		12 49 59.57	+29 29 38.2	12 52 25.00	+29 13 21.0	0.82	CSO176
q1250+3122		12 50 52.87	+31 22 06.3	12 53 17.50	+31 05 50.0	0.78	CSO179
q1250+5650		12 50 15.20	+56 50 37.4	12 52 26.29	+56 34 20.4	0.321	3C277-1=1250+568
q1252+1157		12 52 07.74	+11 57 21.1	12 54 38.20	+11 41 06.1	0.871	PKS1252+11
q1253-0531		12 53 35.89	-05 31 08.3	12 56 01.15	-05 47 21.7	0.538	3C279=1253-055
q1254+0443	ND	12 54 27.51	+04 43 46.6	12 56 59.90	+04 27 34.1	1.024	PG1254+047
q1254+5708	ND	12 54 05.04	+57 08 37.1	12 56 14.20	+56 52 24.0	0.042	MRK231
q1257+2840	ND	12 57 57.79	+28 40 10.6	13 00 22.20	+28 24 01.8	0.092	1257+2840
q1257+3439		12 57 26.64	+34 39 31.4	12 59 48.70	+34 23 22.0	1.375	B2011257+34=1257+346
q1258+2835		12 58 36.56	+28 35 52.3	13 01 00.90	+28 19 44.2	1.355	QSO-1258+285
q1259+5918		12 59 08.26	+59 18 14.6	13 01 12.90	+59 02 06.9	0.472	PG1259+593
q1302-1017		13 02 55.91	-10 17 17.5	13 05 33.00	-10 33 20.4	0.286	PKS1302-102
q1305+0658		13 05 22.57	+06 58 14.2	13 07 53.96	+06 42 14.2	0.602	3C281=1305+069
q1306+3021		13 06 07.27	+30 21 38.1	13 08 29.69	+30 05 39.0	0.806	1306+3021
q1307+0835		13 07 16.27	+08 35 47.4	13 09 47.03	+08 19 49.8	0.155	1307+0835
q1307+4617		13 07 58.59	+46 17 20.8	13 10 11.70	+46 01 24.0	2.129	HS-1307+4617
q1309-0536	ND	13 09 00.76	-05 36 43.7	13 11 36.48	-05 52 38.9	2.188	Q1309-0536
q1309+3531		13 09 58.43	+35 31 15.2	13 12 17.70	+35 15 21.0	0.184	PG1309+355
q1311+0217		13 11 53.60	+02 17 05.7	13 14 26.50	+02 01 14.3	0.306	Q1311+0217
q1317-0142		13 17 15.89	-01 42 20.9	13 19 50.30	-01 58 04.6	0.225	Q1317-0142
q1317+2743		13 17 34.38	+27 43 51.8	13 19 56.30	+27 28 08.4	1.022	TON153=1317+277
q1317+5203		13 17 41.27	+52 03 49.6	13 19 46.23	+51 48 06.1	1.055	1317+5203
q1318+2903		13 18 54.67	+29 03 01.5	13 21 15.80	+28 47 20.0	0.549	TON156
q1318+2903a		13 18 53.58	+29 03 30.5	13 21 14.70	+28 47 49.0	1.703	TON155
q1320+2925		13 20 59.89	+29 25 45.3	13 23 20.50	+29 10 07.0	0.960	TON157
q1321+0552		13 21 48.52	+05 52 42.1	13 24 19.90	+05 37 05.0	0.205	IR1321+0552
q1322+6557		13 22 08.46	+65 57 25.0	13 23 49.50	+65 41 48.0	0.168	PG1322+659
q1323+6530		13 23 48.58	+65 30 47.3	13 25 29.70	+65 15 13.0	1.618	4C65.15
q1327-2040		13 27 24.34	-20 40 48.9	13 30 07.70	-20 56 17.0	1.169	PKS-1327-206-FIX
q1328+3045		13 28 49.74	+30 45 58.6	13 31 08.29	+30 30 32.8	0.849	3C286.0
q1329+4117		13 29 29.82	+41 17 23.7	13 31 41.10	+41 01 59.0	1.93	PG1329+412
q1333+1740		13 33 36.81	+17 40 30.5	13 36 02.00	+17 25 13.0	0.554	PG1333+176
q1334-0033		13 34 13.12	-00 33 41.4	13 36 47.13	-00 48 57.7	2.783	QSO-133647-00485
q1334+2438		13 34 57.34	+24 38 18.2	13 37 18.70	+24 23 03.0	0.108	IR1334+24
q1338+4138		13 38 52.06	+41 38 22.3	13 41 00.77	+41 23 14.1	1.219	1338+416
q1340-0038		13 40 17.51	-00 38 40.8	13 42 51.58	-00 53 46.0	0.326	Q1340-0038
q1340+6036		13 40 30.06	+60 36 48.4	13 42 13.24	+60 21 42.8	0.961	3C288-1
q1346+2637		13 46 29.61	+26 37 13.5	13 48 48.30	+26 22 20.0	0.598	QSO1348+263
q1351+3153		13 51 51.28	+31 53 45.1	13 54 05.39	+31 39 02.4	1.326	B21351+31

Table 1—Continued

Name	Status <sup>a</sup>	RA (1950)	Dec (1950)	RA (2000)	Dec (2000)	<i>z</i>	Alternate Name
q1351+6400		13 51 46.42	+64 00 29.3	13 53 15.86	+63 45 45.6	0.088	PG1351+64
q1352+0106		13 52 25.56	+01 06 51.2	13 54 58.70	+00 52 10.0	1.117	PG1352+011
q1352+1819		13 52 12.60	+18 19 58.9	13 54 35.70	+18 05 17.0	0.152	PG1352+183
q1354+1933		13 54 42.23	+19 33 43.2	13 57 04.50	+19 19 06.6	0.719	PKS1354+19
q1354+2552	ND	13 54 48.35	+25 52 01.5	13 57 06.50	+25 37 25.0	2.032	PKS1354+25
q1355-4138		13 55 57.24	-41 38 20.3	13 59 00.18	-41 52 53.5	0.313	1355-413
q1356+5806		13 56 36.31	+58 06 37.7	13 58 17.60	+57 52 04.4	1.375	4C58-29
q1401+0952		14 01 42.78	+09 52 06.8	14 04 10.60	+09 37 45.5	0.441	1401+0951
q1402+4341	ND	14 02 37.75	+43 41 27.0	14 04 38.79	+43 27 07.3	0.320	Q1402+4341
q1402+2609		14 02 59.34	+26 09 52.2	14 05 16.20	+25 55 33.6	0.164	1402+2609
q1404+2238		14 04 02.52	+22 38 03.2	14 06 21.90	+22 23 47.0	0.098	PG1404+226
q1407+2632		14 07 07.82	+26 32 30.3	14 09 23.88	+26 18 21.2	0.944	PG1407+265
q1408+5642	ND	14 08 14.60	+56 42 36.2	14 09 54.21	+56 28 28.9	2.562	Q1408+5642
q1411+4414	ND	14 11 50.09	+44 14 11.4	14 13 48.30	+44 00 13.0	0.089	PG1411+442
q1413+1143	ND	14 13 20.22	+11 43 38.3	14 15 46.30	+11 29 44.1	2.551	H1413+117
q1415+4343		14 15 03.31	+43 43 55.5	14 17 01.39	+43 30 04.9	0.002	SBS1415+437
q1415+4509		14 15 04.65	+45 09 56.6	14 17 00.91	+44 56 06.0	0.114	PG1415+451
q1416-1256		14 16 21.36	-12 56 58.3	14 19 03.90	-13 10 45.0	0.129	PG1416-129
q1416+0642		14 16 38.80	+06 42 20.2	14 19 08.20	+06 28 34.0	1.436	3C298
q1424-1150		14 24 55.99	-11 50 25.2	14 27 38.10	-12 03 49.9	0.806	PKS1424-118
q1425+2003		14 25 05.80	+20 03 17.1	14 27 25.05	+19 49 52.3	0.111	1425+2003
q1425+2645		14 25 21.93	+26 45 39.3	14 27 35.70	+26 32 15.0	0.366	B21425+26
q1427+4800		14 27 54.04	+48 00 44.1	14 29 43.10	+47 47 26.0	0.221	PG1427+480
q1435-0134		14 35 13.29	-01 34 13.5	14 37 48.30	-01 47 11.0	1.310	Q1435-0134
q1435+6349		14 35 37.30	+63 49 36.3	14 36 45.77	+63 36 38.1	2.068	S4-1435+638
q1439+5343	ND	14 39 02.59	+53 43 03.7	14 40 38.06	+53 30 15.7	0.038	MRK477
q1440+3539		14 40 04.63	+35 39 07.4	14 42 07.46	+35 26 22.9	0.077	1440+3539 MARK-478
q1444+4047		14 44 50.24	+40 47 38.1	14 46 45.91	+40 35 07.1	0.267	PG1444+407
q1451-3735		14 51 18.33	-37 35 24.0	14 54 27.36	-37 47 34.2	0.314	PKS1451-375
q1503+6907		15 03 44.32	+69 07 49.0	15 04 12.70	+68 56 13.0	0.318	B2-1503+691
q1512+3701		15 12 47.42	+37 01 55.7	15 14 43.52	+36 50 51.0	0.371	B2-1512+37
q1517+2356		15 17 08.26	+23 56 53.3	15 19 19.46	+23 46 03.3	1.903	LB9612
q1517+2357		15 17 02.19	+23 57 44.7	15 19 13.39	+23 46 54.4	1.834	LB9605
q1521+1009		15 21 59.93	+10 09 02.9	15 24 24.52	+ 9 58 29.5	1.324	PG1522+101
q1524+5147	ND	15 24 26.04	+51 47 15.5	15 25 53.80	+51 36 49.0	2.860	1524+5147
q1535+5443	ND	15 35 20.75	+54 43 22.0	15 36 38.36	+54 33 33.1	0.039	MRK486
q1538+4745		15 38 00.96	+47 45 10.6	15 39 34.79	+47 35 31.6	0.770	PG1538+477
q1540+1805	ND	15 40 03.58	+18 05 37.5	15 42 19.50	+17 56 07.0	1.662	4C18.43
q1542+5408		15 42 41.88	+54 08 25.6	15 43 59.40	+53 59 03.0	2.371	SBS1542+541
q1544+4855		15 44 00.16	+48 55 25.5	15 45 30.34	+48 46 07.9	0.400	1543+4855
q1545+2101		15 45 31.21	+21 01 27.2	15 47 43.53	+20 52 16.4	0.264	3C323-1=1545+210
q1555+3313		15 55 33.72	+33 13 20.8	15 57 29.95	+33 04 46.7	0.942	B21555+33
q1611+3420		16 11 48.05	+34 20 20.0	16 13 41.10	+34 12 48.0	1.401	DA406=1611+343
q1612+2611		16 12 08.82	+26 11 46.5	16 14 13.23	+26 04 16.2	0.131	1612+2611
q1615+3229		16 15 46.90	+32 29 51.0	16 17 42.50	+32 22 25.0	0.151	3C 332
q1618+1743		16 18 07.37	+17 43 30.5	16 20 21.80	+17 36 24.0	0.555	3C334.0
q1622+2352		16 22 32.30	+23 52 01.3	16 24 39.08	+23 45 12.1	0.927	3C336.0
q1623+2653		16 23 46.05	+26 53 43.4	16 25 48.90	+26 46 59.0	2.526	1623.7+268B

Table 1—Continued

Name	Status <sup>a</sup>	RA (1950)	Dec (1950)	RA (2000)	Dec (2000)	z	Alternate Name
q1626+5529		16 26 51.47	+55 29 04.9	16 27 56.10	+55 22 31.0	0.133	PG1626+554
q1630+3744		16 30 15.18	+37 44 08.3	16 32 01.10	+37 37 49.4	1.478	1630+377
q1631+3930		16 31 19.41	+39 30 41.8	16 33 02.10	+39 24 27.2	1.023	1631+3930
q1634+7037		16 34 51.83	+70 37 37.2	16 34 29.05	+70 31 32.7	1.337	PG1634+706
q1637+5726		16 37 17.53	+57 26 15.8	16 38 13.46	+57 20 23.9	0.745	OS562=1637+574
q1641+3954		16 41 17.67	+39 54 10.8	16 42 58.78	+39 48 36.9	0.595	3C345=1641+399
q1652+3950	ND	16 52 11.85	+39 50 25.2	16 53 52.24	+39 45 36.6	0.033	MRK501
q1656+0519		16 56 05.73	+05 19 47.1	16 58 33.46	+05 15 16.5	0.887	PKS1656+053
q1700+5153	ND	17 00 13.46	+51 53 35.9	17 01 24.90	+51 49 20.0	0.288	PG1700+518
q1700+6416		17 00 40.63	+64 16 24.7	17 01 00.48	+64 12 08.9	2.722	HS1700+6416
q1701+6102	ND	17 01 34.15	+61 02 59.4	17 02 11.11	+60 58 48.0	0.164	1701+6102
q1704+6048		17 04 03.52	+60 48 30.8	17 04 41.30	+60 44 30.0	0.371	3C351.0=1704+608
q1715+5331		17 15 30.33	+53 31 27.2	17 16 35.40	+53 28 16.2	1.940	PG1715+535
q1717+4901		17 17 56.45	+49 01 49.7	17 19 14.53	+48 58 49.6	0.025	ARP102B
q1718+4807		17 18 17.86	+48 07 10.6	17 19 38.30	+48 04 12.2	1.084	PG1718+481
q1803+7827		18 03 39.36	+78 27 54.4	18 00 45.70	+78 28 04.1	0.680	S51803+78
q1821+1042		18 21 41.71	+10 42 45.1	18 24 02.90	+10 44 25.0	1.360	PKS1821+10
q1821+6419		18 21 44.13	+64 19 32.1	18 21 59.40	+64 21 07.5	0.297	E1821+643
q1845+7943		18 45 37.49	+79 43 06.2	18 42 08.80	+79 46 17.0	0.056	3C390.3
q1928+7351		19 28 49.49	+73 51 45.3	19 27 48.50	+73 58 02.0	0.302	4C73.18=1928+738
q1935-6914	ND	19 35 11.88	-69 14 51.3	19 40 25.56	-69 07 56.5	3.152	QSO-194025-69075
q2041-1054		20 41 26.40	-10 54 17.9	20 44 09.76	-10 43 24.5	0.035	MRK509
q2112+0555		21 12 23.47	+05 55 12.9	21 14 52.57	+06 07 42.5	0.457	PG2112+059
q2128-1220		21 28 52.93	-12 20 21.1	21 31 35.42	-12 07 05.5	0.501	PKS2128-12
q2135-1446		21 35 01.25	-14 46 27.4	21 37 45.19	-14 32 55.8	0.200	PKS2135-147
q2141+1730		21 41 13.86	+17 30 02.3	21 43 35.56	+17 43 49.1	0.213	OX1692141+175
q2145+0643		21 45 36.21	+06 43 41.4	21 48 05.50	+06 57 39.0	0.999	PKS2145+067
q2155-3027		21 55 58.38	-30 27 54.4	21 58 52.00	-30 13 32.3	0.116	PKS2155-304
q2200+4202	ND	22 00 39.47	+42 02 08.4	22 02 43.30	+42 16 39.8	0.069	BL-LAC
q2201+3131		22 01 01.58	+31 31 05.3	22 03 15.02	+31 45 37.7	0.297	B22201+31A
q2212-2959		22 12 25.08	-29 59 20.8	22 15 16.00	-29 44 24.0	2.703	PKS2212-299
q2215-0347	ND	22 15 12.21	-03 47 40.6	22 17 47.77	-03 32 39.0	0.241	2215-0347
q2216-0350		22 16 16.52	-03 50 41.0	22 18 52.08	-03 35 37.4	0.901	PKS2216-03
q2223-0512		22 23 11.22	-05 12 17.7	22 25 47.31	-04 57 01.4	1.404	3C446=2223-052
q2230+1128		22 30 07.94	+11 28 22.7	22 32 36.45	+11 43 50.7	1.037	CTA102=2230+114
q2243-1222		22 43 39.85	-12 22 40.0	22 46 18.20	-12 06 51.2	0.630	PKS2243-123
q2251-1750		22 51 25.85	-17 50 54.6	22 54 05.80	-17 34 55.0	0.068	MR2251-178
q2251+1120		22 51 40.67	+11 20 39.5	22 54 10.44	+11 36 38.9	0.323	PKS2251+113
q2251+1552		22 51 29.66	+15 52 54.2	22 53 57.80	+16 08 53.4	0.859	3C454.3=2251+158
q2300-6823		23 00 27.93	-68 23 47.3	23 03 43.50	-68 07 37.1	0.512	PKS2300-683
q2302+0255		23 02 12.10	+02 55 34.0	23 04 44.91	+03 11 45.7	1.052	PG2302+029
q2308+0951		23 08 46.67	+09 51 57.9	23 11 17.81	+10 08 16.2	0.432	PG2308+098
q2340-0339		23 40 22.59	-03 39 05.3	23 42 56.60	-03 22 26.5	0.896	PKS2340-036
q2344+0914		23 44 03.92	+09 14 06.0	23 46 36.90	+09 30 46.0	0.672	PKS2344+092
q2347-4342		23 47 57.40	-43 42 41.0	23 50 34.20	-43 26 00.0	2.90	HE-2347-4342
q2349-0125		23 49 22.28	-01 25 54.9	23 51 56.03	-01 09 13.7	0.174	2349-0125
q2352-3414		23 52 50.76	-34 14 37.5	23 55 25.60	-33 57 55.8	0.706	PKS2352-342

<sup>a</sup>ND: data for this object not analyzed – observation failed, the spectrum contained no signal, data was obtained in SPECTROPOLARIMETRY mode, or the object is a broad absorption line quasar.

Table 2. Observation Details.

Available in:

<http://lithops.as.arizona.edu/~jill/QuasarSpectra/>

or:

<http://hea-www.harvard.edu/QEDT/QuasarSpectra/>.

Table 3. Absorption line lists and line identifications.

Available in:

<http://lithops.as.arizona.edu/~jill/QuasarSpectra/>

or:

<http://hea-www.harvard.edu/QEDT/QuasarSpectra/>.

Table 4. Objects which were only observed Pre-Costar in A-1.

Available in:

<http://lithops.as.arizona.edu/~jill/QuasarSpectra/>

or:

<http://hea-www.harvard.edu/QEDT/QuasarSpectra/>.

Available in:

<http://lithops.as.arizona.edu/~jill/QuasarSpectra/>

or:

<http://hea-www.harvard.edu/QEDT/QuasarSpectra/>.

Fig. 1.— Spectra of quasars obtained with the G130H, G190H or G270H gratings of FOS. The  $1\sigma$  error array is plotted as a dotted line, and the continuum fit is a dashed line. Absorption lines more significant than  $3.5\sigma$  are indicated, for objects whose absorption line spectra have been analyzed. In some cases, absorption line analysis was not carried out (see text). Spectra have been corrected for Milky Way reddening.



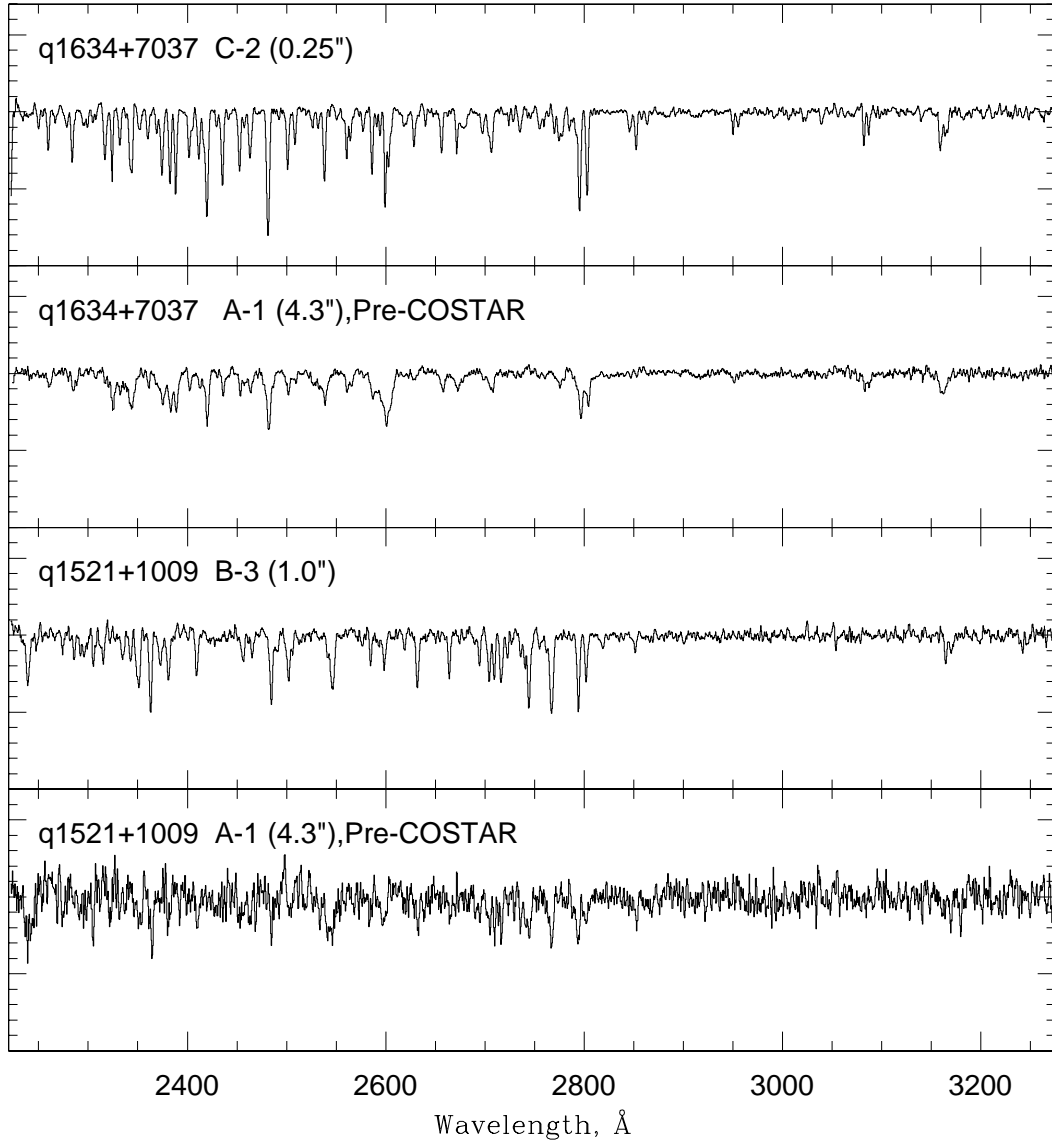


Fig. 2.— Comparison of A-1 Pre-COSTAR and smaller apertures. G270H spectra of Q 1634+7037 and Q1521+1009 obtained through the A-1 (4.3") aperture pre-COSTAR, and the C-2 (0.25 ") and B-3 (1.0 ") apertures, respectively. The spectra have been normalized to unity by the continuum fits.

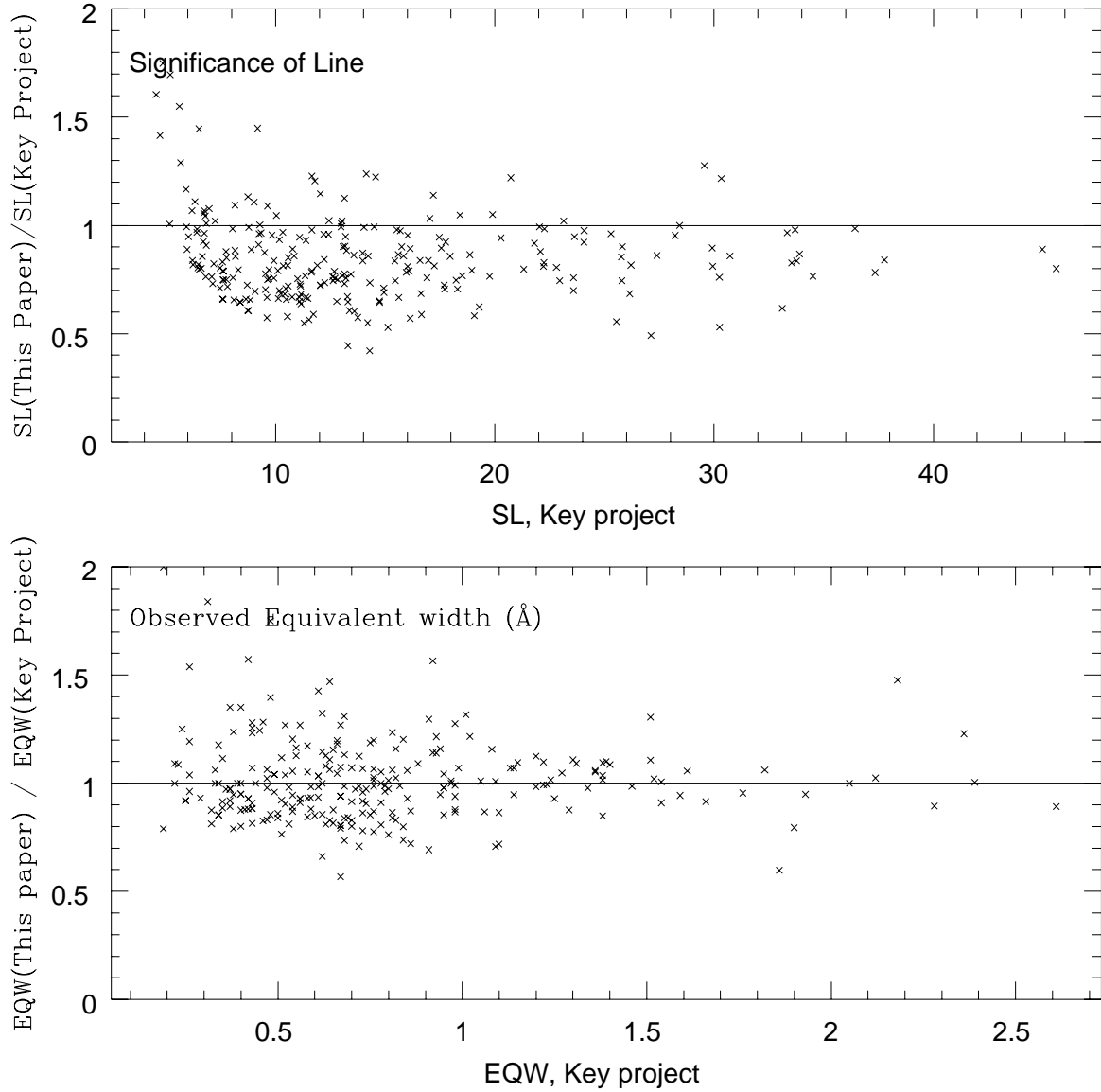


Fig. 3.— Comparison of our line lists with those of the Key Project (J98) for selected objects (see text). Top panel: Ratio of the significance assigned to each line by J98 to that assigned by this work. Lower panel: Ratio of the observed equivalent width of each line measured by J98 to that measured here.